Karlsruhe Institute of Technology

Upward k-Planarity

Bachelor's Thesis of

Franka Fockel

At the Department of Informatics
Institute of Theoretical Informatics (ITI)

Reviewer:	Dr. Torsten Ueckerdt
Second reviewer:	T.T.-Prof. Dr. Thomas Bläsius
Advisors:	Laura Merker
	Samuel Schneider

19.05.2025 – 19.09.2025

Karlsruher Institut für Technologie
Fakultät für Informatik
Postfach 6980
76128 Karlsruhe

The following tools were used to create this thesis:

- ChatGPT-4 and ChatGPT-5 for spelling, grammar and style checking and correction
- ChatGPT-5 for assistance in creating TikZ graphics and looking up LaTeX- commands

---

I declare that I have developed and written the enclosed thesis completely by myself. I have not used any other than the aids that I have mentioned. I have marked all parts of the thesis that I have included from referenced literature, either in their original wording or paraphrasing their contents. I have followed the by-laws to implement scientific integrity at KIT.

Karlsruhe, 19.09.2025

. . . .

(Franka Fockel)

Abstract

A directed acyclic graph (DAG) G is called *upward k-planar* if there exists an embedding Γ of G in the plane such that every edge is a y-monotone Jordan curve and is crossed at most k times. The *upward local crossing number* of a graph G, denoted by $\mathrm{lcr}^{\uparrow}(G)$, is the smallest integer k such that G is upward k-planar.

It is known that $\mathrm{lcr}^{\uparrow}(G) \leq \mathrm{bw}(G)^2$, where $\mathrm{bw}(G)$ denotes the bandwidth of G. We establish improved bounds in the case where G is the Cartesian product of two directed input graphs. For two orientated paths P_1 and P_2 of lengths n_1 and n_2, respectively, we show, by developing suitable embedding techniques, that $\mathrm{lcr}^{\uparrow}(P_1 \square P_2) \in O(\sqrt{\min(n_1, n_2)})$. Moreover, for two DAGs G_1 and G_2, we prove that $\mathrm{lcr}^{\uparrow}(G_1 \square G_2) \in O(\max(\mathrm{bw}(G_1), \mathrm{bw}(G_2))^3)$.

We call a partially ordered set (poset) $\mathcal{P}$ upward k-planar if its Hasse diagram is upward k-planar. We show that there exists no function that bounds the dimension of a poset by its upward local crossing number, nor vice versa.

Zusammenfassung

Ein gerichteter azyklischer Graph (DAG) G wird *upward k-planar* genannt, wenn es eine Einbettung Γ von G in die Ebene gibt, in der jede Kante als y-monotone Jordan-Kurve dargestellt wird und höchstens k Kreuzungen mit anderen Kanten aufweist. Die *upward local crossing number* eines Graphen G, bezeichnet mit $\mathrm{lcr}^{\uparrow}(G)$, ist die kleinste natürliche Zahl k , für die eine solche Einbettung existiert.

Es ist bekannt, dass $\mathrm{lcr}^{\uparrow}(G) \leq \mathrm{bw}(G)^2$ gilt, wobei $\mathrm{bw}(G)$ die sogenannte Bandwidth von G bezeichnet. In dieser Arbeit wird gezeigt, dass sich für das kartesische Produkt zweier gerichteter Graphen durch geeignete Einbettungstechniken verbesserte obere Schranken herleiten lassen. Konkret wird bewiesen, dass für zwei orientierte Pfade P_1 und P_2 der Längen n_1 bzw. n_2 gilt, dass $\mathrm{lcr}^{\uparrow}(P_1 \square P_2) \in O(\sqrt{\min(n_1, n_2)})$. Darüber hinaus zeigen wir für zwei DAGs G_1 und G_2, dass $\mathrm{lcr}^{\uparrow}(G_1 \square G_2) \in O(\max(\mathrm{bw}(G_1), \mathrm{bw}(G_2))^3)$.

Ferner bezeichnet man eine partiell geordnete Menge (Poset) $\mathcal{P}$ als upward k-planar, falls ihr Hasse-Diagramm upward k-planar ist. Es wird gezeigt, dass es keine Funktion gibt, die die Dimension eines Posets durch seine upward local crossing number beschränkt. Ebenso existiert keine Funktion, die die upward local crossing number durch die Dimension des Posets beschränkt.

Contents

1 Introduction

A directed acyclic graph is called *upward k-planar* if it admits an embedding into the plane where every edge is drawn as a y-monotone curve and crossed at most k times. The smallest $k \in \mathbb{N}$ for which such an embedding exists is called the *upward local crossing number* of a graph G. This thesis investigates upward k-planarity for graph classes in which the edge orientation is fixed, with a particular focus on Cartesian products and Hasse diagrams of posets. Our goal is to derive an improved bound for the upward local crossing number of these graph classes by analyzing its relationship to other structural graph parameters.

The notion of upward k-planarity was only recently introduced by Angelini, Biedl, Chimani, Cornelsen, Da Lozzo, Hong, Liotta, Patrignani, Pupyrev, Rutter and Wolff [Ang+25]. It combines the two concepts of *k-planarity* and *upward-planarity*. Graph planarity is a central concept in graph theory. It can be generalized to the notion of *k-planarity*: a graph G is said to be k-planar if it admits a drawing in the plane in which every edge is crossed at most k times. The theory of k-planarity has been studied extensively in the context of "beyond planarity", with a wide range of bounds and structural characterizations (see the survey [DLM19] or books [Bek20 | Sch18]). Seemingly unrelated, we can discuss the notion of upward-planarity for directed graphs. A directed graph is called *upward planar* if it admits a planar embedding, in which every edge is drawn as a y-monotone curve. The question of how it can be determined efficiently whether a directed graph is upward planar is extensively investigated in the literature [DT88 | GT01]. Analogous to the way k-planarity generalizes planarity, upward k-planarity extends the notion of upward planarity.

Angelini et al. show that the upward local crossing number is unbounded for certain planar graph classes, such as bipartite outerplanar graphs. They further show that the upward local crossing number in general has an upper bound that is quadratic in the bandwidth of the graph. They also demonstrate that even for planar graphs, suitable orientations of the edges may force arbitrarily large upward local crossing numbers [Ang+25].

In this thesis, we aim to answer the question of whether the upward local crossing number can also become arbitrarily large for graph classes with fixed edge orientations. While in previous work the local upward crossing number of a graph was analyzed over all possible edge orientations of the graph, we analyze graph classes with already defined, structurally interesting edge orientations and investigate how the given orientation can be used in order to formulate better bounds or influence the analysis of the upward local crossing number of the respective graph, in general. In particular, we study *Cartesian products* of upward k-planar graphs where the edge orientations are determined by the edge orientations of the input graph and formulate a bound that is dependent on the graph parameters of the input graphs and their orientations. Furthermore, we explore the upward local crossing number of posets where the edge direction of the Hasse diagram is also already determined by the partial order of the poset.

Our main results are the following:

- For the Cartesian product of directed paths with arbitrary edge orientations, we show that the number of crossings per edge in an upward embedding has a sublinear upper bound in the length of the shorter path. Corollary 3.20 specifically states that the bound lies in $O(n^{\frac{1}{4}})$ where n is the number of vertices of the Cartesian product. This significantly improves the bound implied by earlier results that state that the upward local crossing number of grids lies in $O(n^{\frac{1}{2}})$ [Ang+25].

- Extending this approach to general Cartesian products, we demonstrate that the number of crossings per edge can be bounded by the maximum bandwidth of both input graphs cubed, i.e., $\max(\text{bw}(G_1), \text{bw}(G_2))^3$; see Corollary 3.25. Previous work states that the upward local crossing number is bounded by the quadratic bandwidth of the Cartesian product [Ang+25]. The bandwidth of the Cartesian product can be bounded by the number of vertices of one input graph times the bandwidth of the other input graph [CDGK75]. If the maximum bandwidth of both input graphs G_1, G_2 is less than the number of vertices of each input graph, this implies an upward bound of the upward local crossing number by $\max(\text{bw}(G_1), \text{bw}(G_2))^4$. Therefore, the result of Corollary 3.25 also improves the known upper bound for the upward local crossing number of Cartesian products.
- Finally, we establish that there exists no function relating the dimension of a poset to its upward local crossing number, and conversely, that the upward local crossing number cannot be bounded by the dimension (Theorem 4.1, Theorem 4.2).

We now give an overview of related work and after that, give an outline of the thesis while formulating the contribution in more detail.

1.1 Related Work

Upward planarity has been a long-standing topic of interest in the context of drawing directed acyclic graphs. Specifically, algorithms to determine whether a graph is upward planar have been studied extensively [DT88 | GT01 | DGL10]. In general, it is NP-complete to determine whether a graph is upward planar [GT01], but there exist graph classes, for example digraphs with additional structural properties, where it can be done in polynomial time [DGL10].

In the context of "Beyond Planarity" the notion of k-planarity and the local crossing number, which describes the maximum number of crossings per edge in an embedding, received considerable attention in graph theory, but largely in isolation from upward planarity [DLM19 | Bek20 | Sch18]. In particular, the local crossing number of undirected Cartesian Products of cycles, stars, paths and small planar graphs is analyzed in detail [Mus19]. Furthermore, the crossing number, which describes the sum of all crossings of an embedding, has been investigated for special undirected Cartesian products with paths [Asi+24] and for certain undirected poset-related structures such as the hypercube [SV91].

The unified concept of upward k-planarity for directed acyclic graphs was only introduced recently by the paper mentioned above. In addition to the already mentioned results, it shows that testing upward k-planarity is NP-complete, even for graph classes where upward planarity testing can be solved in polynomial time. For a graph G with maximum degree Δ and bandwidth $\text{bw}(G)$ it is established that the upward local crossing number lies in $O(\Delta \cdot \text{bw}(G)) \subseteq O(\text{bw}(G)^2)$. Based on known bandwidth bounds for certain graph classes, they obtain more specific results: for $k \times k$ grids, the upward local crossing number is $O(k)$, while for planar graphs with maximum degree Δ and n vertices, it is in $O\left(\frac{n \cdot \Delta}{\log_\Delta(n)}\right)$. They also show that not every acyclic *fan* is upward planar, and there are directed acyclic graphs of pathwidth 2 with the number of vertices and the maximum degree in $O(k)$ that are not k-planar.

Moreover, classical results in combinatorics establish relationships between upward planarity and the dimension of posets [TM77 | BFR72]. They specifically state that if a poset has a unique greatest element or a unique smallest element and the Hasse diagram is planar, the dimension is at most 3. If the poset has a unique greatest element and a unique smallest element and the Hasse diagram is planar, the dimension is at most 2.

1.2 Detailed Contribution and Outline

In Chapter 2, necessary definitions and concepts from graph theory and combinatorics are introduced.

In Chapter 3, we study the upward local crossing number of Cartesian products of two directed acyclic graphs.

In Section 3.1, we develop upper bounds for simple cases of Cartesian products. We present first insights into the upward local crossing number of Cartesian products of two paths that include at least one monotone directed path: Theorem 3.3 states that these Cartesian products admit an upward planar embedding. We further establish that, for the cubic Cartesian product of monotone paths, the upward local crossing number has a linear upper bound in the length of the shortest input path, see Corollary 3.5.

In Section 3.2, we develop general embedding techniques for Cartesian products and use these to derive an upper bound for the Cartesian product of an arbitrarily orientated path and a directed acyclic graph. The bound presented in Corollary 3.14 depends linearly on the bandwidth and maximum degree of the input DAGs. We also formulate a bound based on certain structural properties of the orientated path solely, which is done in Lemma 3.16 and Lemma 3.17. We then show in Lemma 3.19 that the bandwidth of an orientated path with length $n-1$ is in $O(\sqrt{n})$ and conclude in Corollary 3.20 that the upward local crossing number of the Cartesian product of two paths also lies in $O(\sqrt{n})$ with n being the length of the shorter path. We extend this embedding approach to general Cartesian products and obtain an upper bound depending polynomially on the bandwidth of the input graphs in Corollary 3.25.

In Section 3.3, we turn to lower bounds for the upward local crossing number of Cartesian products of paths. We identify in Theorem 3.26 and Theorem 3.27 structural conditions under which upward planar embeddings are impossible.

Finally, in Chapter 4, we construct counterexamples showing that there is no general relationship between the upward local crossing number of a poset's Hasse diagram and the dimension of the poset.

In Chapter 5 we summarize our results and outline directions for future research on upward k-planarity for certain graph classes and posets.

2 Preliminaries

We begin by introducing notation and concepts that will be used throughout this thesis.

2.1 Basic Definitions and Notation

Let G be a graph with a finite vertex set. We refer to the vertex set of G with $V(G)$ and to the edge set of G with $E(G)$. Unless explicitly stated otherwise, all graphs in this thesis are directed graphs without loops or multi-edges. For a directed edge $(u, w) \in E(G)$ we also write uw and call u and w *adjacent*.

Two graphs G and H are *isomorphic*, written $G \simeq H$, if there exists a bijection between $V(G)$ and $V(H)$ that preserves adjacency.

If $V' \subseteq V(G)$, the subgraph *induced* by V' is the graph H with vertex set $V(H) = V'$ and edge set $E(H) = \{uw \in E(G) \mid u, w \in S\}$. The graph $G - V'$ is defined as the subgraph induced by $V(G) \setminus V'$ subgraph of G. If $E' \subseteq E(G)$, the subgraph induced by E' is the graph that has E' as an edge set and all incident vertices to E' as a vertex set. The graph $G - E'$ is defined as $(V(G), E(G) \setminus E')$. Given a directed graph G, its *underlying undirected graph* G' has the same vertex set and adjacency relation as G, but all edges are undirected.

A graph G is *connected* if for all $u, v \in V(G)$ there exists a path between u and v in the underlying undirected graph. A graph is k*-connected* if $G - W$ is connected for all vertex sets $W \subseteq V(G)$ with $|W| \leq k$. A *cut* is the partition of the vertex set into disjoint subsets. All edges that have exactly one endpoint in each subset of the partition are referred to as the *cut-set* and we say that this edge set *induces the cut.*

For a vertex $v \in V(G)$, the *in-degree* is

$$d_{\text{in}}(v) = |\{(u, v) \in E(G) \mid u \in V(G)\}|,$$

and the *out-degree* is

$$d_{\text{out}}(v) = |\{(v, u) \in E(G) \mid u \in V(G)\}|.$$

A vertex v with $d_{\text{in}}(v) = 0$ is called a *source*, while a vertex with $d_{\text{out}}(v) = 0$ is called a *sink*. The *degree* of a vertex v is defined as $d(v) = d_{\text{in}}(v) + d_{\text{out}}(v)$. The *maximum degree* of a graph G is

$$\Delta(G) \coloneqq \max_{v \in V(G)} d(v).$$

2.2 Embeddings and Upward k-Planarity

An *embedding* Γ of a graph G maps every vertex $u \in V(G)$ to a distinct point in the plane and every edge $e \in E(G)$ to a continuous Jordan curve $f_e : [0, 1] \to \mathbb{R}^2$ such that $f_e(0)$ and $f_e(1)$ are the positions of its endpoints. The set $f_e((0, 1))$ is called the set of *inner points* of e. If for two distinct edges $e, e' \in E(G)$ the sets $f_e((0, 1))$ and $f_{e'}((0, 1))$ intersect, we say that e and e' *cross.* In this thesis, we only consider embeddings where no vertex is placed on the interior of an edge, no edge crosses itself, any two edges cross at most once, and no three edges cross in a common point.

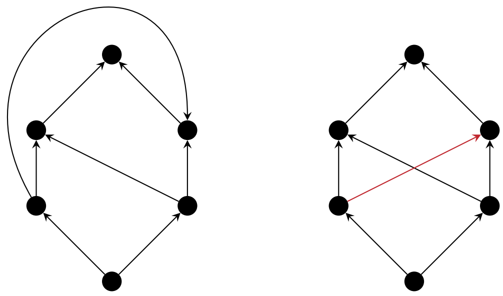

Figure 2.1: This figure illustrates that not every planar graph, see embedding on the left, has also an upward planar embedding. The given graph is upward 1-planar [Ang+25].

The *local crossing number* of an embedding Γ, denoted $\mathrm{lcr}(\Gamma)$, is the maximum number of crossings per edge. The total number of crossings is the *crossing number* of Γ, denoted $cr(\Gamma)$. The (local) crossing number of a graph G is defined as the minimum (local) crossing number over all embeddings, denoted $\mathrm{lcr}(G)$ and $\mathrm{cr}(G)$, respectively.

An embedding Γ is called *k-planar* if $\mathrm{lcr}(\Gamma) \leq k$. A graph G is called *k-planar* if it admits a k-planar embedding. If an embedding (or graph) is 0-planar, we simply call it *planar*.

Lemma 2.1: *Let Γ be an embedding of a graph G. Then*

$$\mathrm{lcr}(\Gamma) \;\geq\; \frac{2}{|E(G)|} \cdot \mathrm{cr}(\Gamma).$$

Proof. Assume every edge $e \in E(G)$ is crossed strictly less than $\frac{2}{|E(G)|} \cdot \mathrm{cr}(\Gamma)$ times. Summing over all edges and dividing by two for the fact that every crossing consists out of two edge, the total number of crossings would then be strictly less than $\mathrm{cr}(\Gamma)$, contradicting the definition of $\mathrm{cr}(\Gamma)$. ∎

An embedding is called *upward* if every edge is represented by a y-monotone curve. Not every directed graph admits such an embedding: in particular, any graph containing a directed cycle does not admit one. Therefore, we only consider *directed acyclic graphs (DAGs)*, i.e. directed graphs without directed cycles. As illustrated in Figure 2.1 not every planar graph is also upward planar.

An embedding is *upward k-planar* if it is both upward and k-planar.

Definition 2.2: *The* upward local crossing number *of a directed acyclic graph G, denoted $\mathrm{lcr}^{\uparrow}(G)$, is the minimum local crossing number over all upward embeddings of G.*

Clearly, it holds for every directed graph G that $\mathrm{lcr}^{\uparrow}(G) \geq \mathrm{lcr}(G)$.

There are a few other properties and concepts concerning embeddings that are used throughout this thesis. For a planar embedding Γ of a graph G, a *face* is a connected region of $\mathbb{R}^2 \setminus \{f_e([0,1]) \mid e \in E(G)\}$. The unbounded region is the *outer face*, and the remaining regions are the *internal faces*. The edges whose curves are incident to a face f are called the *boundary edges* of f. If a vertex v is incident to a boundary edge of f, then we say v *lies on* f. If v lies on f but has no incoming boundary edges, v is a *source of* f.

The *convex hull* of Γ, denoted $\mathrm{con}^{\circ}(\Gamma)$, is the smallest convex set $M \subseteq \mathbb{R}^2$ that contains all vertex positions and all curves representing edges.

We define the coordinate projections

$$\pi_x : \mathbb{R}^2 \to \mathbb{R}, \quad (x, y) \mapsto x, \qquad \pi_y : \mathbb{R}^2 \to \mathbb{R}, \quad (x, y) \mapsto y.$$

For an embedding Γ, the *projection onto the x-axis* is $\pi_x(\mathrm{con}^{\circ}(\Gamma))$; the projection onto the y-axis is $\pi_y(\mathrm{con}^{\circ}(\Gamma))$.

An embedding is called *straight-line* if every edge is represented by a line segment, i.e. for every $e \in E(G)$ $f_e([0,1])$ is contained in a straight line. It is called *linear* if all vertices share the same x- or y-coordinate.

Finally, we define two families of graphs used throughout this thesis: A *path* on n vertices is an undirected graph that is isomorphic to $(\{1, \dots, n\}, \{\{i, i+1\} \mid 1 \leq i < n\})$. The *length* of the path is the number of edges. The *complete bipartite graph $K_{m,n}$* is an undirected graph that is isomorphic to the graph $(A \cup B, \{\{a, b\} \mid a \in A,\ b \in B\})$ with $|A| = m$, $|B| = n$, and $A \cap B = \emptyset$.

2.3 Posets

For Chapter 4 we introduce a number of definitions and basic concepts concerning partially ordered sets and their notation.

A *partially ordered set (poset)* is a pair $\mathcal{P} = (P, E)$ with $E \subseteq P \times P$ such that E is

- reflexive: $(x, x) \in E$ for all $x \in P$,
- transitive: if $(x, y) \in E$ and $(y, z) \in E$, then $(x, z) \in E$ for all $x, y, z \in P$,
- antisymmetric: if $(x, y) \in E$ and $(y, x) \in E$, then $x = y$ for all $x, y \in P$.

If $(x, y) \in E$ we also write $x \leq y$ and say that x is *smaller than* y, or y is *greater than* x. If $x \leq y$ and $x \neq y$, we write $x < y$. A poset $\mathcal{P}$ is *finite* if P is a finite set; in this thesis, we only consider finite posets.

Two elements $x, y \in P$ are *comparable* if $x \leq y$ or $y \leq x$. Otherwise x and y are *incomparable*, denoted b< $x \parallel y$. An element $x \in P$ is called a *minimal element* if no $y \in P$ satisfies $y < x$, and a *maximal element* if no $y \in P$ satisfies $x < y$. A poset is called *bounded* if it has both a unique minimal and a unique maximal element. The unique minimal or maximal element is often denoted by 0 or 1, respectively. The *downset* of an element x, denoted by $D(x)$, is defined as $D(x) := \{y \in P \mid y < x\}$.

The element $z \in P$ is a *meet* of $x, y \in P$ if $z \leq x, z \leq y$ and z is maximal among all such elements. The element $z \in P$ is a *join* of x, y if $x \leq z, y \leq z$ and z is minimal among all such elements. If every pair of elements in $\mathcal{P}$ has a unique meet and join, then $\mathcal{P}$ is a *lattice*.

For $x, y \in P$, we say that x *covers* y if $y < x$ and there is no $z \in P$ with $y < z < x$. The *Hasse diagram* of a poset $\mathcal{P}$ is the directed graph with vertex set P and edges (y, x) whenever x covers y, drawn in the plane so that all edges are y-monotone Jordan curves. Thus, the Hasse diagram can be seen as an upward embedding of the graph $(P, \{(y, x) \mid x \text{ covers } y\})$.

A poset $\mathcal{Q} = (Q, \leq_Q)$ is a *subposet* of $\mathcal{P} = (P, \leq_P)$ if $Q \subseteq P$ and $x \leq_Q y$ implies $x \leq_P y$ for all $x, y \in Q$. A poset $\mathcal{L} = (L, \leq_\ell)$ is a *linear extension* of $\mathcal{P} = (P, \leq_P)$ if $\mathcal{P}$ is a subposet of $\mathcal{L}$ and every two elements of L are comparable under $\leq_\ell$. The *intersection* of two posets $\mathcal{P}_1 = (P, \leq_1)$ and $\mathcal{P}_2 = (P, \leq_2)$ is $\mathcal{P}_1 \cap \mathcal{P}_2 = (P, \leq)$ where $x \leq y$ if and only if $x \leq_1 y$ and $x \leq_2 y$.

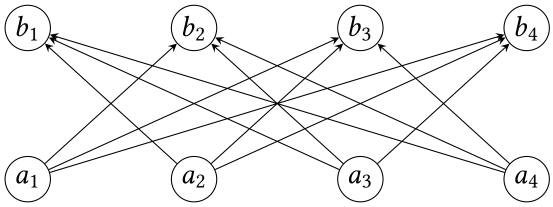

Figure 2.2: This illustrates the standard example S_4.

The *(Dushnik-Miller-)dimension* of a poset $\mathcal{P}$, denoted $\dim(\mathcal{P})$, is the smallest integer n for which there exist linear extensions $\ell_1, \dots, \ell_n$ such that

$$\ell_1 \cap \dots \cap \ell_n = \mathcal{P}.$$

This dimension concept was introduced by Dushnik and Miller in 1941 [DM41]. For every subposet $\mathcal{Q}$ of $\mathcal{P}$, it holds that $\dim(\mathcal{Q}) \leq \dim(\mathcal{P})$.

Finally, the so-called *standard example* S_n is the poset

$$S_n = \big(\{a_1, \dots, a_n\} \cup \{b_1, \dots, b_n\}, \{(a_i, b_j) \mid 1 \leq i, j \leq n,\ i \neq j\}\big).$$

S_4 is illustrated in Figure 2.2.

3 Cartesian Products and Upward k-Planarity

In this chapter we analyze the upward local crossing number of Cartesian products and formulate improved upper bounds for the Cartesian Product of paths as well as for the Cartesian Products in general. Furthermore, we investigate the structural properties of Cartesian Products of paths that cannot be embedded upward planar.

We begin by examining basic products of graphs in order to explore some first arguments concerning upward planar embeddings. In particular, we start by focussing on the Cartesian product of (directed) paths that admit an upward planar embedding. More complex graph products and their embedding properties are in subsequent sections.

All Cartesian products examined in the first section contain a directed path component in which all edges are orientated consistently in the same direction. An example of such a path of length 5 is illustrated in Figure 3.1.

We refer to such paths as *(monotone) directed paths* and define them in the formal, following way: An orientation of a path with vertex set $\{1, \ldots, n\}$, $n \in \mathbb{N}$ is said to be *(monotone) directed* if its vertices can be labeled such that each edge is of the form $(i, i+1)$ for all $i \in \{1, \ldots, n-1\}$.

Paths with arbitrary edge orientation are referred to as orientated paths. In contrast to orientated paths, monotone paths on m vertices are indicated by an arrow, specifically as $\vec{P_m}$.

Although upward planar embeddings for arbitrary paths are generally easy to obtain, we emphasize that every path admits an upward planar embedding in which the x-coordinates of the vertices strictly increase along the underlying undirected path. We refer to such embeddings as *x-unique*. An example of a x-unique embedding, alongside an embedding that does not satisfy this requirement, is illustrated in Figure 3.2.

Lemma 3.1: *Every orientated path admits an upward planar embedding in which the x-coordinates of the vertices strictly increase with increasing vertex index, and all vertex coordinates lie in $\mathbb{Z} \times \mathbb{Z}$.*

Proof. Given an orientated path P with length $n \in \mathbb{N}$, we construct an embedding in which all vertices are assigned to integer coordinates with strictly increasing x-coordinates along the path and show that this embedding is upward planar.

We label the vertices of P as $\{0, \ldots, n\}$, such that the labels increase along the underlying undirected path. The vertex with label 0 is placed at the origin. Now, we construct the rest of the embedding.

We construct the embedding by traversing the path in label order. Suppose vertex $i \in \{1, \ldots, n\}$ has neighbor $i-1$ already embedded at coordinates (x_{i-1}, y_{i-1}). Then we embed vertex i at (x_i, y_i), where $x_i = x_{i-1} + 1$, and

$$y_i = \begin{cases} y_{i-1} + 1, & \text{if } (i-1, i) \in E(P), \\ y_{i-1} - 1, & \text{if } (i, i-1) \in E(P). \end{cases}$$

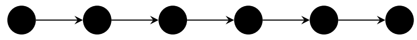

Figure 3.1: Example for a (monotone) directed path with length 5, denoted by $\vec{P}_6$.

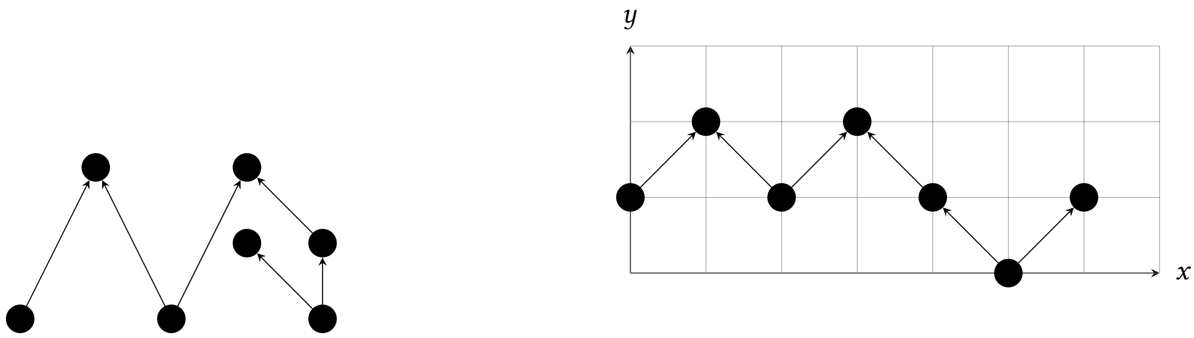

(a) P **(b)**

Figure 3.2: Two embeddings of an orientated path P are shown. The embedding in Figure 3.2a does not satisfy the properties stated in Lemma 3.1, whereas the embedding in Figure 3.2b is constructed according to the steps of the proof of Lemma 3.1 and satisfies all required properties.

All edges are drawn as straight-line segments.

By induction on i, we observe that $x_i = i$ for all i, so the x-coordinate strictly increases along the vertex labels. Moreover, all vertex coordinates lie in $\mathbb{Z} \times \mathbb{Z}$.

Next, we show that the embedding is upward. For any edge $e \in E(P)$, we have $e = (i-1, i)$ or $e = (i, i-1)$ for some i. In the cases that e connects $(i-1, y_{i-1})$ to (i, y_i), we always have $y_i = y_{i-1} + 1 > y_{i-1}$. Otherwise, if e connects (i, y_i) to $(i-1, y_{i-1})$ then $y_i = y_{i-1} - 1 < y_{i-1}$ by construction. Therefore, all edges are embedded in an upward direction.

We discuss planarity next. For this, recall that each vertex lies at a unique integer coordinate in $\mathbb{Z} \times \mathbb{Z}$. The inner points of all edges lie in $(\mathbb{R} \setminus \mathbb{Z}) \times (\mathbb{R} \setminus \mathbb{Z})$. For any edge e connecting vertex i to $i+1$, the x-coordinate of its inner points lies strictly between i and $i+1$. Since there are n edges and n such non-overlapping intervals on the x-axis, no two edges share the same x-interval. So, no two edges can cross in their inner points. Hence, the embedding is planar.

Since this construction can be applied to any orientated path and the resulting embedding is both upward and planar, the claim is proven. ∎

Now we introduce the Cartesian product of directed graphs as a method to construct new graphs.

Definition 3.2 (Cartesian product of directed graphs)**:** *Let G_1, G_2 be arbitrary graphs with a set of vertices $V(G_i)$ and an edge set $E(G_i)$ for $i \in \{1, 2\}$. The* Cartesian product of G_1 and G_2, *denoted by $H = G_1 \,\square\, G_2$, is defined by*

$$V(H) := V(G_1) \times V(G_2),$$

$$E(H) := E_1(H) \cup E_2(H),$$

where $E_i(H)$ represents the vertex relation $\sim_i$, $i \in 1, 2$:

$$(u_1, u_2) \sim_1 (v_1, v_2) \iff (u_1, v_1) \in E(G_1) \wedge u_2 = v_2$$

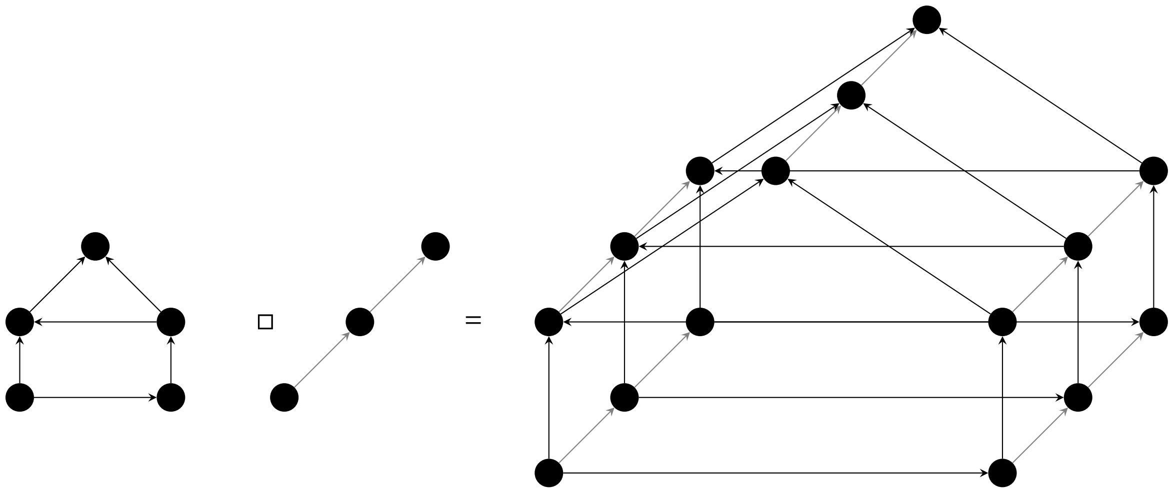

Figure 3.3: The Cartesia product $H = G \,\square\, \vec{P}_3$ of a graph G and a monotone directed path $\vec{P}_3$: The edges of $E_G(H)$ are colored black and induce three copies of G, whereas the edges of $E_{\vec{P}_2}$ are colored thick gray and induce $5 = |V(G)|$ copies of $\vec{P}_3$.

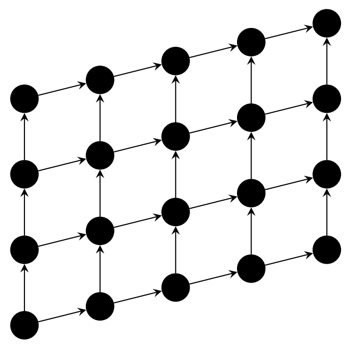

Figure 3.4: This figure illustrates an upward planar embedding of the Cartesian product of $\vec{P}_4$ and $\vec{P}_5$. The Cartesian product of other monotone paths can be embedded in a similar way, also yielding upward planar embeddings.

$$(u_1, u_2) \sim_2 (v_1, v_2) \iff u_1 = v_1 \wedge (u_2, v_2) \in E(G_2).$$

with G_1 being the first and G_2 being the second input graph.

It is easy to see that the subgraph of H induced by $E_1(H)$ consists of pairwise disjoint $|V(G_2)|$ copies of G_1 and the subgraph of H induced by $E_2(H)$ consists of $|V(G_1)|$ copies of G_2. This observation is illustrated in Figure 3.3. In general, for Cartesian product H we refer to the edge set $E_i(H)$ as the edges inducing pairwise disjoint copies of the ith input graph or for an input graph G with the edge set $E_G(H)$ to the edges inducing pairwise disjoint copies of G.

Moreover, depending on the input graph G we can describe $E_G(H)$ in more detail. For example, if one of the input graphs of the Cartesian product is a monotone directed path on m vertices and the other input graph an arbitrary graph G, we can describe one edge subset as

$$E_{\vec{P}_m}(H) = \{((i, v), (i+1, v)) \mid i \in \{1, \dots, m-1\}, v \in V(G)\}.$$

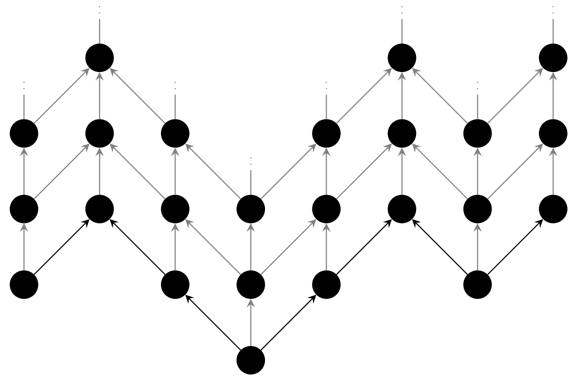

Figure 3.5: Part of the Cartesian product of an arbitrary orientated graph P and a monotone directed path $\vec{P}_n$. The black edges highlight a x-unique embedding of P. The pattern gets repeated depending on n.

3.1 Upper Bounds for Cartesian Products With Monotone Paths

In order to become familiar with the Cartesian product and its characteristics, we show a simple first result concerning upward planarity of the Cartesian product of two directed paths. The Cartesian product of two monotone directed paths $\vec{P}_4$ and $\vec{P}_5$ is illustrated in Figure 3.4. Observe, that the Cartesian product of two monotone paths is always upward planar. By using the result of Lemma 3.1 we can generalize this observation and make a statement concerning the upward planarity of the Cartesian product of a monotone directed path and an arbitrarily orientated path. An example for such an Cartesian product is given in Figure 3.5, already using the embedding proposed in the proof of the following statement.

Theorem 3.3: *The Cartesian product $G = \vec{P}_n \square P_m$, $m, n \in \mathbb{N}$ of a monotone directed path $\vec{P}_n$ and an arbitrary orientated path P_m is upward planar.*

Proof. Given a monotone directed path $\vec{P}_n$ with $n \in \mathbb{N}$ vertices and some other orientated path P_m with $m \in \mathbb{N}$ vertices we construct an embedding for $G = \vec{P}_n \square P_m$ that is both planar and upward. An example of this construction is shown in Figure 3.5.

According to Lemma 3.1, every orientated path admits an upward planar embedding in which all vertices and inner edge points have distinct x-coordinates. We choose such an embedding for P_m.

Next, we construct n copies of this embedding of P_m, each translated by one unit in the y-direction relative to the previous one. Then, for every pair of vertically aligned vertices in successive layers — i.e., vertices sharing the same x-coordinate and differing by one unit in the y-coordinate—we add an upward edge connecting them. Observe that with this we created an embedding of $G = \vec{P}_n \square P_m$.

We now verify the upwardness of this embedding. By construction, all edges in $E_{\vec{P}_n}$—which connect vertices across adjacent layers—are explicitly drawn upward. The edges in E_{P_m} forming each a copy of the x-unique embedding of P_m are also upward due to Lemma 3.1. Since every edge in G belongs to either $E_{\vec{P}_n}$ or E_{P_m}, the overall embedding is upward.

Next, we prove that it is also planar. We discuss possible crossings within the two defined edge subsets first and take a look at crossings between them afterward.

We start with $E_{\vec{P}_n}$, which are the edges added between the copies of P_m. Each edge in $E_{\vec{P}_n}$ lies in $\mathbb{Z} \times \mathbb{R}$ and is a vertical segment of unit length. These edges are translated copies of the segment from $(0, 0)$ to $(0, 1)$ and thus do not cross each other.

Next, we analyze the other edge subset E_{P_m} to show that there are no crossings between two edges that are both in E_{P_m}. Every edge $e \in E_{P_m}$ lies within a copy of P_m whose embedding ensures planarity within that copy.

The only potential crossings with other edges P_m would be with edges sharing the at least one x-coordinate from another copy. However, since each copy of P_m is a vertical translation of the same embedding and the original embedding of P_m prohibits two edges from sharing an x-coordinate, no such conflicting edge exists. Thus, edges from different copies of P_m are pairwise non-crossing.

Lastly, we discuss whether an edge $e \in E_{P_m}$ crosses an edge from $E_{\vec{P}_n}$. Observe, that the inner points of e lie in $(\mathbb{R} \setminus \mathbb{Z}) \times (\mathbb{R} \setminus \mathbb{Z})$, which implies that e can only intersect an edge from $E_{\vec{P}_n}$ at one of its endpoints, since the coordinates of the inner points of the edges in $E_{\vec{P}_n}$ lie in $\mathbb{Z} \times (\mathbb{R} \setminus \mathbb{Z})$. We conclude that this embedding of $G = \vec{P}_n \square P_m$ is both upward and planar. ■

3.1.1 The Cubic Cartesian Product of Monotone Paths

After discussing some basic results on the Cartesian product of two paths, we extend the concept to Cartesian product involving more than two input graphs and derive an upper bound for the upward local crossing number for the Cartesian product of three monotone paths, building on the insights developed in the previous section.

We define the ternary Cartesian product as follows:

$$G_1 \square G_2 \square G_3 := (G_1 \square G_2) \square G_3 = G_1 \square (G_2 \square G_3).$$

Before addressing the Cartesian product of three monotone directed paths of arbitrary lengths, we begin with a simpler case: the ternary Cartesian product of a monotone path with itself, what already allows us to discuss the core ideas and challenges.

Theorem 3.4: *For every graph $G = \vec{P}_n \square \vec{P}_n \square \vec{P}_n$, where $\vec{P}_n$ denotes a monotone directed path of on $n \in \mathbb{N}$ vertices, there exists an upward $(n-1)$-planar embedding of G.*

Proof. Similar to the proof in Section 3.1 given a monotone path on n vertices with vertex set $V(\vec{P}_n) = \{0, \dots, n-1\}$ we introduce a construction in order to embed the Cartesian product and proof that the constructed embedding is upward $(n-1)$-planar, i. e. that all edges are upward and that there is no edge with more than $(n-1)$ crossing.

We embed each vertex $(i, j, k) \in V(G) = V(\vec{P}_n)^3$ at the coordinate $(i \cdot n + k, j \cdot n + k)$, and represent all edges as straight-line segments between the coordinates of their respective endpoints. This embedding for $\vec{P}_4$ and the context of the coordinates is illustrated in Figure 3.6.

Before discussing the characteristics of the embedding, we introduce some notation similar to the beginning of Chapter 3 in order to structure our argumentation and get some intuition for the embedding itself. We partition the edge set $E(G)$ into three disjoint subsets $E_1(G), E_2(G), E_3(G)$. $E_1(G)$ is given by

$$E_1(G) = \{((i, j, k), (i+1, j, k)) \mid i \in \{0, \dots, n-1\},\ j, k \in \{0, \dots, n\}\},$$

and $E_2(G)$ and $E_3(G)$ are defined analogously with respect to the second and third coordinates. Observe that $E_1(G)$ holds all the horizontal, $E_2(G)$ all the vertical and $E_3(G)$ all the diagonal embedded edges.

We start by discussing the upwardness of the embedding. With the described construction and Figure 3.6, it is easy to observe that if we rotate the embedding around the bisector of the positive x- and y-axes by an angle $0 < \alpha < \pi/2$, then every edge becomes upward.

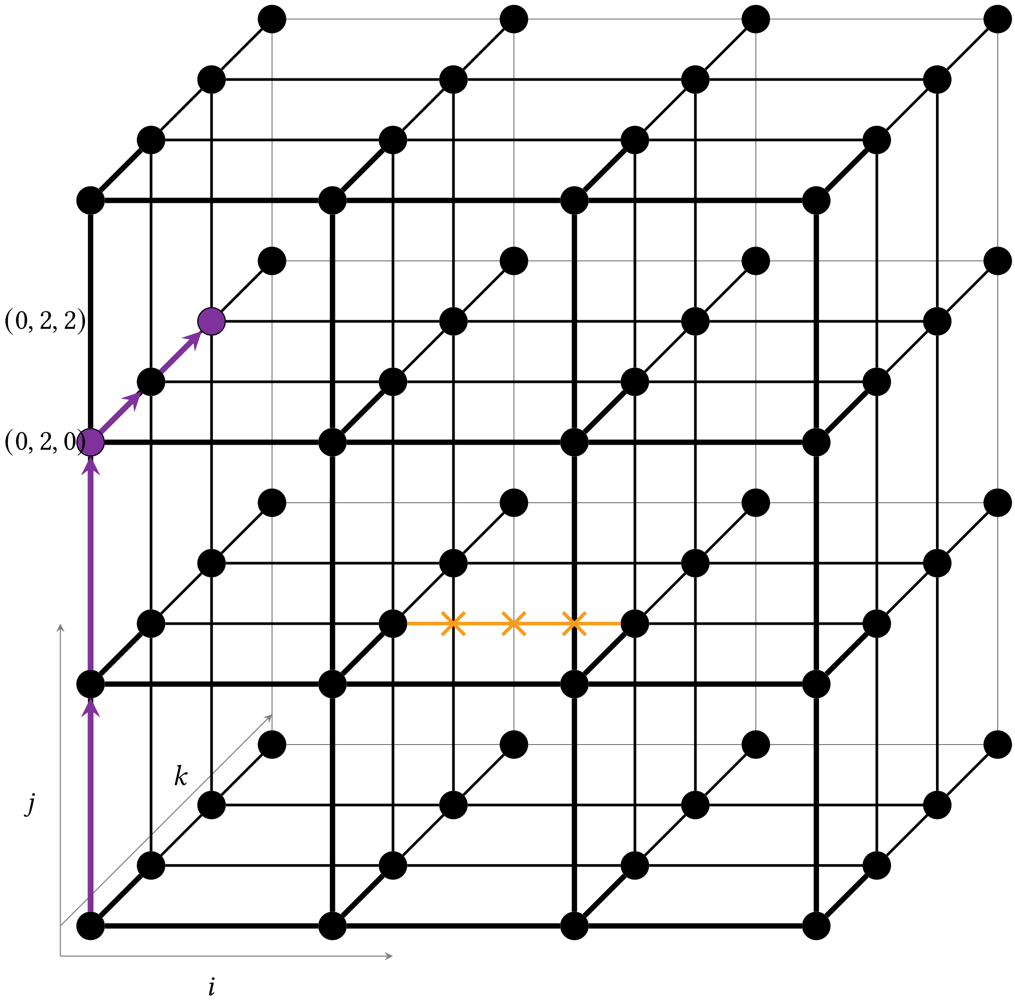

Figure 3.6: An upward 3-planar embedding of $G = \vec{P}_4 \square \vec{P}_4 \square \vec{P}_4$. We can interpret it as four copies of the grid $\vec{P}_4 \square \vec{P}_4$ with each cell of the grid big enough to contain a diagonal version of $\vec{P}_4$. All vertices inside one copy of the grid $\vec{P}_4 \square \vec{P}_4$ have therefore a distance of at least n. If we want to determine the coordinates of a vertex $(0, 2, 2)$, we can find the vertex $(0, 2)$ in the foremost grid, highlighted, and then follow the incident path embedded two steps into the adjacent cell and reach $(0, 2, 2)$, highlighted violet. So the coordinates of $(0, 2, 2)$ are those of the vertex $(0, 2)$ plus the vector $(2, 2)$ for traversing the diagonal $k = 2$ steps, meaning the coordinates are $(0 \cdot 4 + 2, 2 \cdot 4 + 2) = (2, 10)$. The orange highlighted edges illustrates all crossing opportunities from vertical edges with integer coordinates.

Already ensuring the upwardness, we now discuss the planarity, ignoring any possible rotation. In order to do so, we determine between which edge subsets potential crossings can occur. First, we analyze whether edges from the same subset cross each other. As already observed, edges in $E_1(G)$ are always horizontal, each of length exactly n and therefore a translation of the edge connecting the origin to $(n, 0)$. Thus, edges in $E_1(G)$ do not cross each other. Analogously, edges in $E_2(G)$ are also translations of one another and do not cross each other. The same argument holds for $E_3(G)$

It is left to show whether edges from different subsets do cross each other. The edges in $E_3(G)$ are neither crossed by edges from $E_1(G)$ or $E_2(G)$, since the edges of $E_3(G)$ as diagonal edges between adjacent integer coordinates have no inner points with integer coordinates. We conclude that every edge $e \in E_3(G)$ is crossing-free.

Now, we take a look at the edge set $E_1(G)$, which holds all the horizontal edges. Since all edges in $E_3(G)$ are crossing-free, they do not cross edges from $E_1(G)$ and we already established that edges from $E_1(G)$ do not cross other edges from $E_1(G)$. Thus, an edge $e \in E_1(G)$ can only be crossed by edges from $E_2(G)$, i.e. can only be crossed by vertical edges.

In order to bound the number of crossings with vertical edges we count the inner coordinates where crossings can occur. Since the x- coordinates of edges from $E_2(G)$ are always integer crossings can only occur at integer-coordinates. Also because the set $E_2(G)$ is crossing-free within itself, there can only be one crossing per integer-coordinate. The horizontal edge e has length n and therefore $n + 1$ integer-coordinates, two of those are endpoints, leaving $n - 1$ inner integer-coordinates, where crossings can occur. Consequently, the edge e is not crossed by more than $n - 1$ other edges. The situation is also illustrated in Figure 3.3.

An analogous description holds for a vertical edge $e' \in E_2(G)$, which can only be crossed by horizontal edges of $E_1(G)$ up to $n - 1$ times.

Since the rotation described earlier does not change the crossing number, and no edge is crossed more than $n - 1$ times, the rotated embedding is upward $(n - 1)$-planar. ∎

After establishing the main arguments for k-planarity and upwardness for this type of embedding of the cubic Cartesian products of monotone paths with the same length, we now consider Cartesian products of monotone paths with differing lengths. As observed previously, the number of crossings is strongly influenced by the length of the path that is embedded diagonally, since it defines the length of the vertical and horizontal edges and therefore number of integer coordinates from $E_1(G)$ and $E_2(G)$. Taking this into account, we construct a corresponding embedding that accommodates paths of arbitrary lengths. An example of such a Cartesian product is illustrated in Figure 3.7.

Corollary 3.5: *For every graph $G = \vec{P_m} \square \vec{P_n} \square \vec{P_p}$, where each $\vec{P_k}$ denotes a monotone directed path on $k \in \{m, n, p\} \subset \mathbb{N}$ vertices, there exists an upward $(\min(m, n, p) - 1)$-planar embedding of G.*

Proof. Given three monotone directed paths $\vec{P_m}, \vec{P_n}, \vec{P_p}$ with $m, n, p \in \mathbb{N}$ and without loss of generality $p = \min(m, n, p)$, we embed the Cartesian product $G = \vec{P_m} \square \vec{P_n} \square \vec{P_p}$ dependent on p, such that it is upward $(p - 1)$-planar.

Similar to the proof of Theorem 3.4, we embed each vertex $(i, j, k) \in V(G)$ at the coordinate $(i \cdot p + k, j \cdot p + k)$ with $i \in \{0, \dots, m - 1\}, j \in \{0, \dots, n - 1\}, k \in \{0, \dots, p - 1\}$, and represent all edges as straight-line segments between the coordinates of their respective endpoints. Applying the same arguments as in the proof of Theorem 3.4, we conclude the desired properties for this embedding. ∎

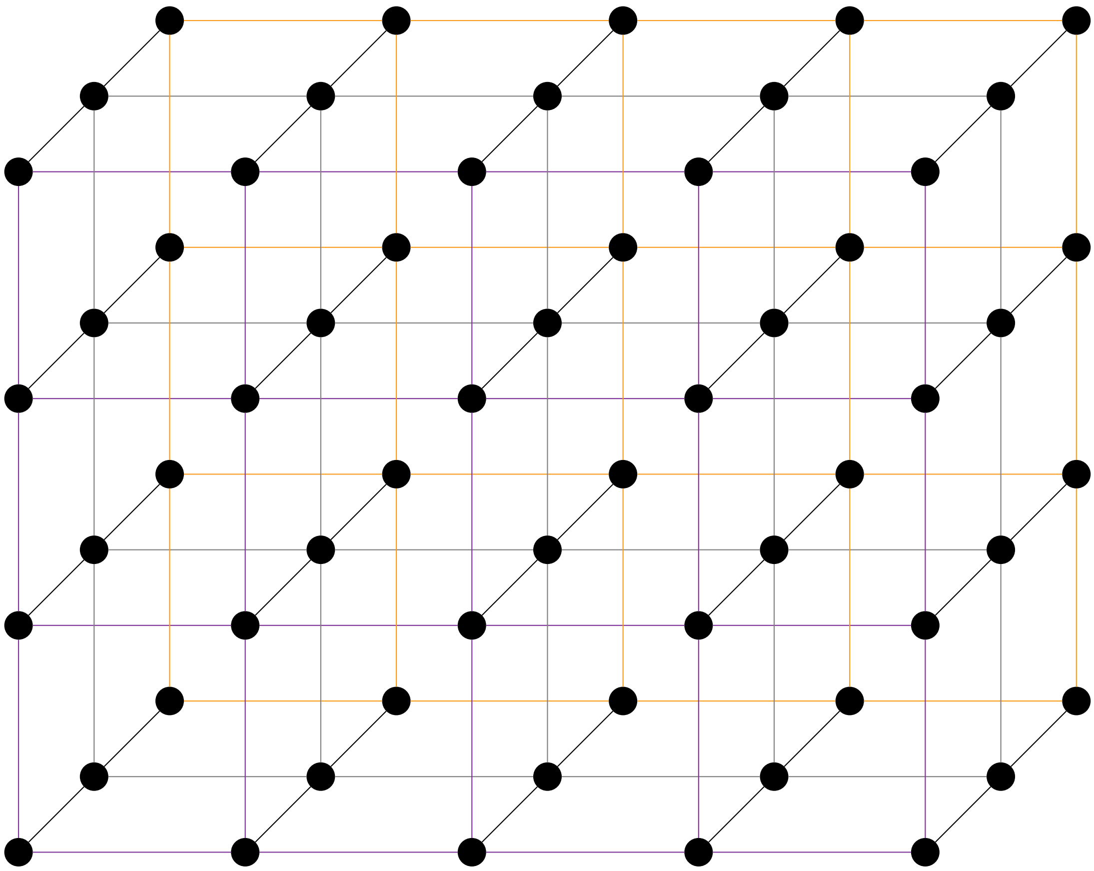

Figure 3.7: An upward 2-planar embedding of $G = \vec{P}_5 \square \vec{P}_4 \square \vec{P}_3$. The edges are colored for a clearer arrangement. Observe that in order to minimize crossings, the shortest path has to be embedded diagonal.

3.2 Upper Bounds for Cartesian Products

In this section, we formulate upper bounds for the upward local crossing number Cartesian Products depending on the input graphs by transmitting the simple results of Section 3.1 onto more complex scenarios, namely substituting the monotone directed path by an arbitrarily orientated path as an input graph and generalizing it for two arbitrary input graphs afterward. There is a special focus on the Cartesian Product of two arbitrary orientated paths, where we derive bounds dependent on the orientation of the paths, which results in an improved bound. In contrast to before, we do not always embed edges as straight line segments in this section. We introduce basic embedding techniques and additional graph parameters in order to argue for the bounds.

3.2.1 Embeddings of Cartesian Products

Before discussing Cartesian products of more complex graphs we introduce some terminology in order to describe general embedding techniques. An embedding into the Euclidean plane is characterized by the position of the vertices and Jordan curves representing the edges. We call two embeddings equivalent if the *planarization* of the embeddings are equivalent. The planarization of an embedding Γ of a graph G describes a planar embedding of the graph G' derived from G by replacing all crossings in Γ with vertices.

Recall the edge partition of the edges of a Cartesian product we introduced in the beginning of Chapter 3. The edge set $E_{G_1}(G_1 \square G_2)$ holds all the edges that induce copies of G_1. G_1*-edges* refers to the same set of edges.

There are numerous approaches to embed the Cartesian product of two graphs into the Euclidean plane. We introduce an embedding technique that depends on given embeddings of the input graphs. An example is illustrated in Figure 3.8.

For a graph $G = G_1 \square G_2$ and embeddings Γ_{G_1} of G_1 and Γ_{G_2} of G_2, the $\Gamma_{G_1}(\Gamma_{G_2})$*-embedding* of G refers to the following construction: We begin with the embedding Γ_{G_1} of G_1, focusing only on the vertex positions. It is possible to modify this embedding such that each vertex can be replaced by a copy of Γ_{G_2}, with the property that the minimal enclosing spheres of these copies are pairwise disjoint. This process yields an embedding of the vertices of $G = G_1 \square G_2$, where a vertex $(i, j) \in V(G)$, for $i \in \{0, \dots, |V(G_1)| - 1\}$ and $j \in \{0, \dots, |V(G_2)| - 1\}$ is embedded as the j-th vertex of the i-th copy of G_2 (replacing the former i-th vertex of the adapted embedding of G_1). All G_2-edges in each copy appear as they are embedded in Γ_{G_2}. In order to complete the construction of this embedding the embedding of the G_1-edges still has to be defined. A G_1-edge e connects vertices from two different G_2-copies. Those copies correspond to vertices $v, w \in V(G_1)$ in Γ_{G_1}. We embed e as a scaled version of Jordan curve representing the edge $e' = (v, w) \in E(G_1)$ in Γ_{G_1}. With this, we have characterized the position of the vertices as well as the Jordan curves representing the edges and therefore created a well-defined embedding of $G = G_1 \square G_2$. The $\Gamma_{G_2}(\Gamma_{G_1})$-embedding of the vertices of G is constructed analogously. For comparison, the minimal example from Figure 3.8 is used again in Figure 3.9 but this time the roles of the input graphs and their embeddings are swapped.

We can identify an embedding as a $\Gamma_{G_1}(\Gamma_{G_2})$-embedding with the following formal definiton.

Definition 3.6: *Given two graphs G_1, G_2 and embeddings Γ_{G_1} of G_1 and Γ_{G_2} of G_2, we call an embedding of the Cartesian product $G_1 \square G_2$ an $\Gamma_{G_1}(\Gamma_{G_2})$-embedding if*

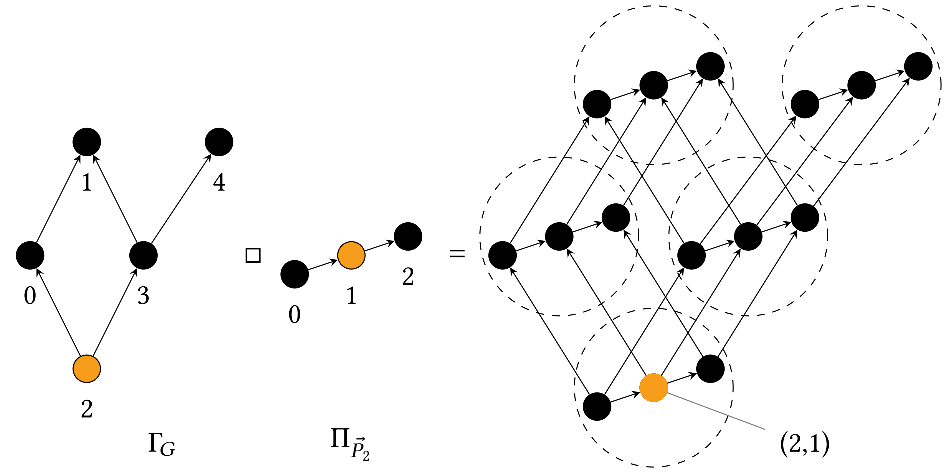

Figure 3.8: On the right: the Cartesian product of the graph G and $\vec{P}_2$, with a straight-line $\Gamma_G(\Pi_{\vec{P}_2})$-embedding of vertices and edges. On the left: the respective embeddings of the input graphs with labeled vertices. We observe that the minimal enclosing spheres, as well as the individual copies of $\vec{P}_2$ in the embedded product, do not intersect. The vertex $(2, 1)$ is highlighted.

- *all induced copies of G_2 are embedded as in Γ_{G_2},*
- *the convex hulls of the copies of G_2 within the embedding of the product do not intersect and*
- *all induce copies of G_1 are embedded equivalent to Γ_{G_1}.*

We call an embedding $\Gamma_{G_1}(\cdot)$-embedding, if only the last two requirements are met.

An important observation is the following: In a $\Gamma_{G_1}(\cdot)$-embedding of G edges within individual copies of G_2 do not cross edges from other G_2-copies. If there are two upward planar input graphs, even more possible crossings are prevented.

Lemma 3.7: *Let G_1 and G_2 be upward planar graphs. For upward planar embeddings $\Gamma_{G_1}, \Gamma_{G_2}$ of G_1 and G_2 a $\Gamma_{G_1}(\Gamma_{G_2})$-embedding of the Cartesian product $G_1 \square G_2$ satisfies the following properties:*

- *the set of G_2-edges is crossing-free,*
- *each copy of G_1 in G induces a crossing-free embedding and*
- *the embedding is upward.*

Proof. We analyze the given embedding concerning the desired properties by analyzing the G_2-edges and G_1-edges after one another.

We start with the G_2-edges, which by construction, appear exactly as in Γ_{G_2}. Since Γ_{G_2} is upward planar, these edges do not cross within their respective copies and are upward. Furthermore, since the minimal enclosing spheres of the embedded copies are disjoint, no edge within one copy can cross an edge from another copy. Consequently, the set of G_2-edges is crossing free and we satisfied the first property.

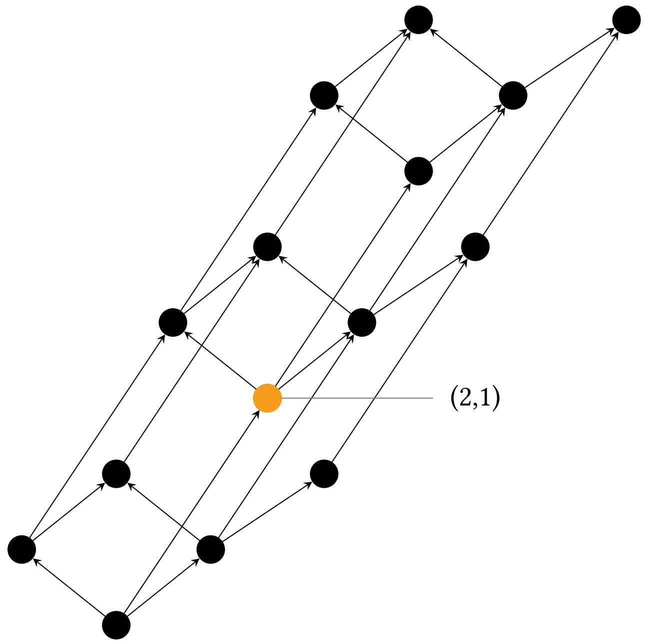

Figure 3.9: The Cartesian product of the graph G from Figure 3.8 and $\vec{P}_2$, with a straight-line $\Pi_{\vec{P}_2}(\Gamma_G)$-embedding of vertices and edges. The vertex $(2,1)$ is highlighted, again.

Next, we verify that each copy of G_1 embedded within $G_1 \square G_2$ is itself crossing free. By construction, each such copy is a scaled version of Γ_{G_1}. Since scaling and translation preserve planarity and upwardness, the embedding of each G_1-copy retains the upward planar properties of the original and therefore there are no crossings between the edges of one copy.

Finally, we observed that both edge sets only contain upward edges and we can conclude the last property. ■

According to Di Battista and Tamassia [DT88], there also exists a straight-line embedding of G_1 that is upward planar. If we use this embedding instead of Γ_{G_1} we can also ensure that for each edge $e \in E(G_1)$ the copies of e do not cross each other.

In contrast to the property of G_2-edges stated in Lemma 3.7, G_1-edges from different copies of G_1, may cross each other (and vice versa if it is an $\Gamma_{G_2}(\cdot)$-embedding instead), as we can see in Figure 3.8 and Figure 3.9.

There are two restrictions whose application is interesting in order to analyze potential crossings in the embedding of a Cartesian product.

One restriction is to require that edges belonging to the copies of G_1 are not allowed to cross edges from the copies of G_2; that is, the only crossings, aside from those internal to the copies themselves, may occur between edges from different copies of G_1. Those crossing are referred to as G_1-crossings.

An alternative restriction is to require that edges in the copies of G_1 are not allowed to cross through other copies of G_1. Thus, crossings may only occur between edges belonging to $E_1(G)$ and $E_2(G)$. These are called (G_1, G_2)-crossings.

So, one restriction states that there are no (G_1, G_2)-crossings, whereas the other forbids G_1- and G_2-crossings.

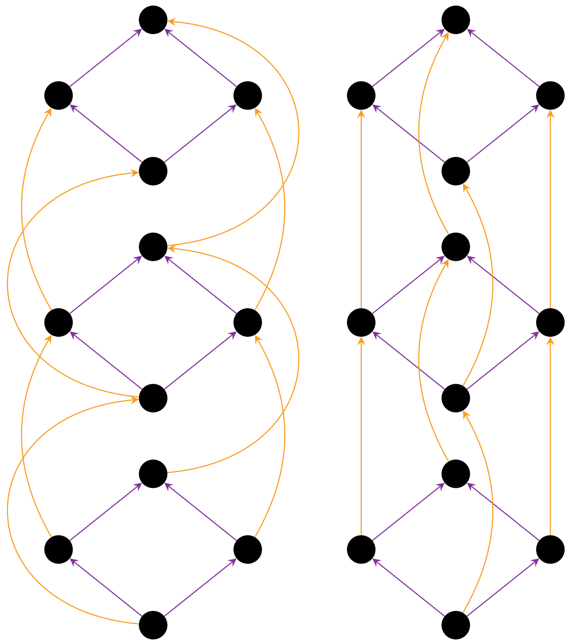

Figure 3.10: Both edge restriction applied to the same product structure of a monotone path P and a graph G. On the left there are only P-crossings. On the right there are only G-P-Crossings and no G-Crossings. The G-edges are highlighted violet and the P-edges are orange.

In order to illustrate both restrictions, we use the a $\vec{P}_2(\cdot)$-embedding of the Cartesian product of $\vec{P}_2$ and a graph G, but change the edge embedding, accordingly. The result is presented in Figure 3.10. Observe, that the properties of Lemma 3.7 still hold. This distinction can significantly affect the resulting upward local crossing number.

We can state, that with a fitting embedding of the vertices the first restriction can always be met.

Lemma 3.8: *For every two graphs G and H there exists an upward embedding of the Cartesian product $G \square H$ without (G, H)-crossings.*

Such an embedding for the product from Figure 3.10 is presented in Figure 3.11. Observe, that this embedding is not interesing for us because the upward local crossing number is big.

Proof. We construct a fitting embedding using linear embeddings. We choose upward embeddings of G and H, denoted by Γ and Θ, where all vertices have the same x-coordinate and every edge in Γ is embedded on the left side of the spine, whereas every edge in Θ is embedded on the right side of the spine. We construct an $\Gamma(\Theta)$-embedding of the Cartesian product. Due to construction all vertices have the same x-coordinate and form a vertical line, with the G-edges on the left side and the H-edges on the right side. Therefore there are no (G, H)-crossings. ∎

Analogous to the first restriction, the second restriction can also always be satisfied if we create a fitting vertex embedding and the input graphs are upward planar. Otherwise crossings within one copy and therefore the whole edge set are not preventable.

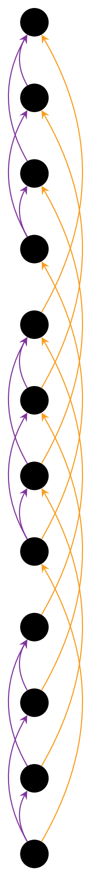

Figure 3.11: Embedding without crossings between G-edges (violet) and H-edges (orange).

Lemma 3.9: *For every two upward planar graphs G and H there exists an embedding of the Cartesian product $G \square H$ without G- and without H-crossings.*

To illustrate the embedding process, Figure 3.13 shows the same Cartesian Product as Figure 3.12 but without G- and H-crossings.

Proof. We construct an embedding using special upward planar embeddings of the input graphs Γ_G and Γ_H, such that there are no crossings within the G- or within H edges.

We start by specifying these special embeddings. We choose Γ_G as an upward planar embedding of G, where every vertex has a unique x-coordinate. Furthermore we choose Γ_H as an upward planar embedding, where every vertex has a unique y-coordinate. Such embedding always exists, since we can take an arbitrary embedding and alter the vertex position by some small translation vector and create an equivalent embedding with unique x- or y-coordinates of the vertices. Now we alter both embeddings to new embeddings Γ'_G and Γ'_H by increasing the distance between the respective vertices such that we can replace each vertex in Γ'_G by a copy of Γ'_H such that projection of the convex hulls of these copies onto the x-axis are not intersecting (and the other way around, i.e. replacing the each vertex in Γ'_H by a copy of Γ'_G where the projection of the convex hull onto the y-axis should be non intersecting).

We use these embeddings to create a $\Gamma'_H(\Gamma'_G)$-embedding of the product graph.

Now, we check for potential crossings between and within copies of the same graph. Note that since the vertices of Γ_H (and therefore Γ'_H) have unique y-coordinates it is possible to assign each copy of G their own layer, i. e. interval on the y-axis, as they replace the original vertices in the construction. Since every copy has their own layer, the copies do not cross each other. Every Γ'_H-copy is induced by vertices that have the same position in each Γ'_G-copy and since in Γ'_G every vertex can by replaced by a copy of Γ'_H without there convex hulls projected on the x-axis intersecting, we can assign every copy of H their own interval on the x-axis which implies that the H-copies also do not cross other H-copies. This is also illustrated in Figure 3.13 Due to the planarity of Γ_G and Γ_H there are no crossings within a copy, either. So, there are no crossings within the H- or G-edges and the only possible crossings must appear between G- and H-edges. ∎

We observe that an alternative proof can be found by proving that the created embedding is a $\Gamma_G(\cdot)$-embedding according as well as $\Gamma_H(\cdot)$-embedding according to Definition 3.6. Then Lemma 3.7 leads to the result, immediately. The described embedding in the proof of Lemma 3.9 will be relevant in Section 3.2.2 and Section 3.2.3 and is referred to as the *canonical* (Γ_G, Γ_H)-*embedding*.

3.2.2 The Cartesian Product With One Arbitrarily Orientated Path

In this subsection, we analyze Cartesian products where one of the input graphs is a path, but not necessarily a monotone path. We discuss different embedding techniques introduced in Section 3.2.1 in order to explore possible upper bounds for the $lcr^{\uparrow}$ of the Cartesian product of a graph G with an embedding Γ and an orientated path P.

We first motivate why Cartesian products with arbitrarily orientated paths do not admit intuitive embeddings that minimise the upward local crossing number. A naive approach to embedding the Cartesian product of P and G would be a $\Pi(\Gamma)$-embedding with an x-unique embedding Π of P, similar to Figure 3.9. However, since P is not necessarily monotone, this construction introduces not only (P, G)-crossings as already observed in Figure 3.9, but also up to $|V(G)|$ additional P-crossings for a single P-edge.

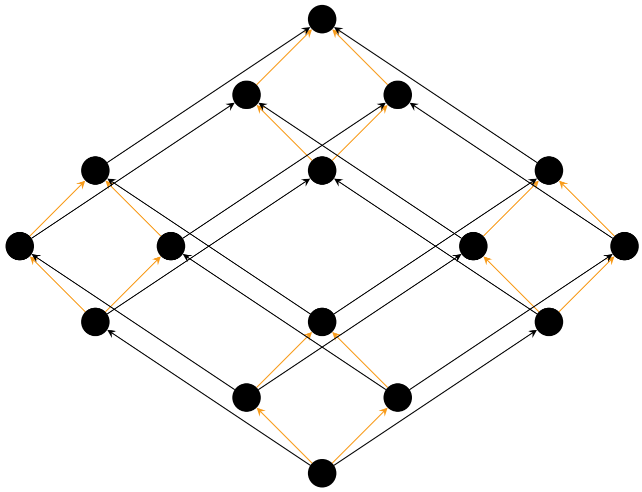

Figure 3.12: Embedding of the Cartesian product of the graphs $G = H = (\{0,1,2,3\}, \{(0,1),(0,2)(1,3),(2,3)\})$. The G-edges are orange and the H-edges are black. Observe that there are H-crossings.

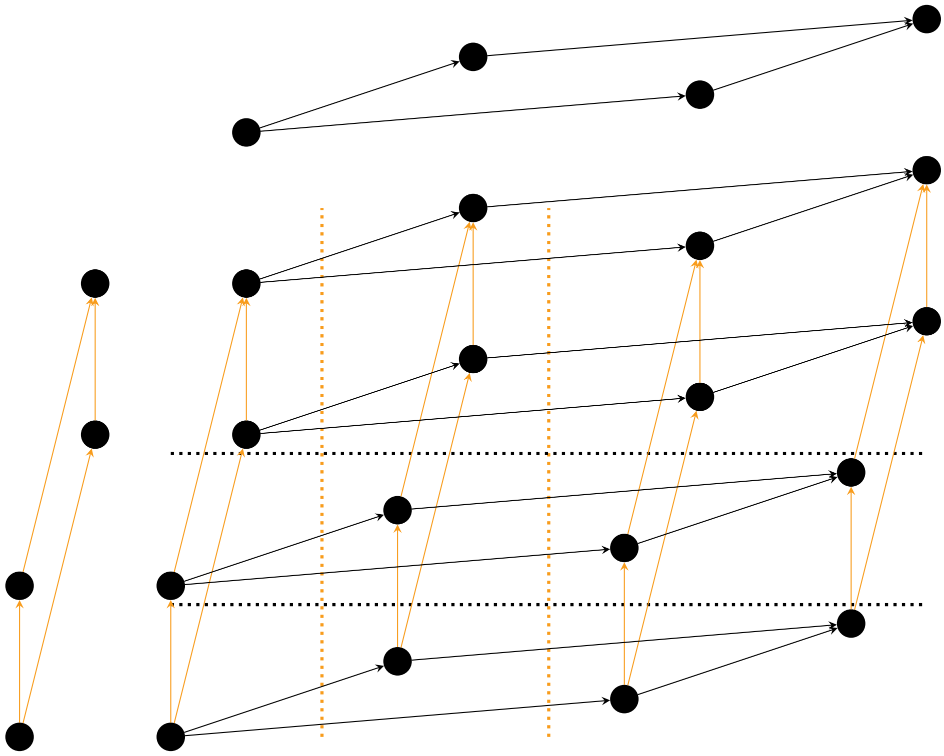

Figure 3.13: Embedding of the same Cartesian product as in Figure 3.12, but this time the construction is based on the proof of Lemma 3.9 and therefore there are no G-crossings (between the orange edges) or H-crossings (crossings between the black edges). The dotted lines illustrate the layers of the of the G-copies on the x-axis or of the H-copies on the y-axis. The Figure also illustrates that the embedding of the product could be an $\Gamma(\cdot)$-embedding with Γ being the embedding on the left or at the top, as well.

Alternatively, one could use a $\Gamma(\Pi)$-embedding similar to Figure 3.8, which avoids all P-crossings. Nevertheless, as illustrated in Figure 3.8, there can still be up to $|V(P)|$ crossings for a single G-edge. In both cases, the next natural idea can be to stack the copies of one input graph and route the edges of the other input graph around these copies. However, this only reduces the number of P-crossings or G-crossings, respectively, by a factor of $\frac{1}{2}$, and the upward local crossing number remains linear in the number of vertices of at least one input graph. This contrasts with the monotone case, where we have already established that an upward planar embedding of the Cartesian product exists.

To address this problem, we aim to construct embeddings that explicitly depend on the orientation of one of the input graphs. The key idea is that the closer a path's orientation resembles a monotone path, the fewer crossings should occur in its Cartesian product with another orientated path or with another graph. We see that the canonical embedding for special embeddings of the input graphs could be a fitting embedding technique to enforce this behavior and the crossings can be described easily.

The approach presented here relies on two structural parameters of the input graphs: their *cutwidth* and *bandwidth*. In the theorems that follow, we show in particular that for paths both parameters can be expressed in terms of the orientation of their edges.

To define these parameters formally, we first introduce the concept of a linear ordering of the vertices of a graph. An ordering φ of a graph G is a bijection from $V(G)$ to the set $\{0, 1, \ldots, n-1\}$, where $n = |V(G)|$, and $\varphi(v)$ is called the *label* of v. We denote by $\Phi(G)$ the set of all such orderings of G. If G is a directed graph we say φ is a topological ordering if $\varphi(u) < \varphi(w)$ for all $(u, w) \in E(G)$. Then, $\Phi(G)$ is defined as the set of all topological orderings of G. The length of an edge $uw \in E(G)$ with respect to an ordering φ is defined as the difference of the labels of their endpoint $|\varphi(u) - \varphi(w)|$.

The *bandwidth* of an ordering φ is defined as the length of the longest edge in the ordering. The *cutwidth* of an ordering φ is the smallest integer k such that all cuts of the ordering, i.e., partitions of the ordering into two subsets with subsequent labels, are crossed by at most k edges.

Formally, these quantities are given by:

$$\mathrm{bw}(\varphi, G) := \max_{(u,w)\in E(G)} |\varphi(u) - \varphi(w)|$$

$$\mathrm{cw}(\varphi, G) =: \max_{v\in V(G)} |\{uw \in E(G) \mid \varphi(u) < \varphi(v) \leq \varphi(w)\}|.$$

The bandwidth of G is then defined as

$$\mathrm{bw}(G) = \min_{\varphi\in\Phi(G)} \mathrm{bw}(\varphi, G)$$

and the cutwidth of G as

$$\mathrm{cw}(G) = \min_{\varphi\in\Phi(G)} \mathrm{cw}(\varphi, G).$$

Note, that this definition ensures that for the bandwidth and cutwidth of directed graphs only topological orderings matter. If its is clear from the context that φ is an ordering of G we sometimes write $\mathrm{bw}(\varphi)$ instead of $\mathrm{bw}(\varphi, G)$.

In the following, we observe that the cutwidth of every ordering of a graph G is bounded by its bandwidth.

Lemma 3.10: *Let G be a graph and φ an ordering of G. Then* $\mathrm{cw}(\varphi, G) \leq \Delta(G) \cdot \mathrm{bw}(\varphi, G)$.

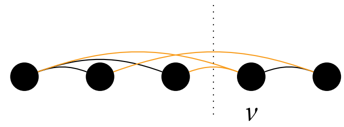

Figure 3.14: The cut between the vertex v and its predecessor in the ordering is illustrated as a dotted line. All edges in the ordering that cross this cut are highlighted in orange; collectively, these edges form the set U_v.

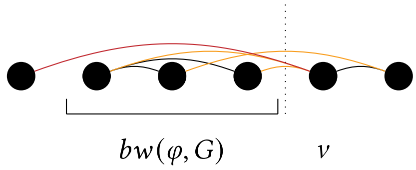

Figure 3.15: The edge colored in red is an edge that crosses the cut at v and is therefore an element of U_v, while its starting vertex at a distance greater than $\mathrm{bw}(\varphi, G)$ from v in the ordering. Hence, the length of the edge is greater than $\mathrm{bw}(\varphi, G)$, which contradicts the definition of the bandwidth itself.

Proof. Let G be a graph and let φ be an ordering of its vertices. Recall that the cutwidth of an ordering φ is the smallest integer k such that every cut that partitions the ordering into two subsets with subsequent labels is crossed by at most k edges.

Let $v \in V(G)$ be an arbitrary vertex with label $\varphi(v)$. We show that the cut between v and the vertex with label $\varphi(v) - 1$ is crossed by at most $\Delta(G) \cdot \mathrm{bw}(\varphi, G)$ edges, where $\Delta(G)$ denotes the maximum degree of G. This cut is illustrated in Figure 3.14.

To formalize this, let us define the set of edges crossing the cut at v as $U_v := |\{uw \in E(G) \mid \varphi(u) < \varphi(v) \leq \varphi(w)\}|$. These are precisely the edges with one endpoint on each side of the cut.

Note that, for every edge $uw \in U_v$, the smaller of the two labels, say $\varphi(u)$, differs from $\varphi(v)$ by at most $\mathrm{bw}(\varphi, G)$. Otherwise, the length of uw would exceed the bandwidth, since $\varphi(w) \geq \varphi(v)$. This is illustrated in Figure 3.15.

Thus, the edges in U_v originate from at most $\mathrm{bw}(\varphi, G)$ vertices lying to the left of v, and each of these vertices has degree at most $\Delta(G)$. Hence, the number of such edges is bounded by $|U_v| \leq \Delta(G) \cdot \mathrm{bw}(\varphi, G)$ and therefore we have that $\mathrm{cw}(\varphi, G) \leq \Delta(G) \cdot \mathrm{bw}(\varphi, G)$. ∎

We restrict our attention to topological orderings of the vertices in order to define the *upward local crossing number* of orderings. In a linear ordering, two edges are said to cross if their endpoints alternate in the ordering.

The *upward local crossing number* of a topological ordering φ of a graph G, denoted by $\mathrm{lcr}^{\uparrow}(\varphi, G)$, is the smallest integer k such that no edge is crossed more than k times in φ. We can establish an upper bound for the upward local crossing number in terms of the bandwidth $\mathrm{bw}(G)$.

Lemma 3.11: *Let G be a directed acyclic graph and φ a topological ordering of G. Then* $\mathrm{lcr}^{\uparrow}(\varphi, G) \leq \Delta(G) \cdot (\mathrm{bw}(\varphi, G) - 1)$.

Proof. Let G be a directed, acyclic graph and φ be a topological ordering of its vertices. We aim to show that every edge $e = (u, w) \in E(G)$ is crossed at most $\Delta(G) \cdot (\mathrm{bw}(\varphi, G) - 1)$ times in the ordering φ.

Recall that two edges in a linear ordering cross if their endpoints alternate. Thus, an edge $e' \in E(G)$ crosses e if and only if it has exactly one endpoint v satisfying $\varphi(u) < \varphi(v) < \varphi(w)$, i.e., exactly one of its endpoints lies between the endpoints of e in the ordering.

By the definition of bandwidth, there are at most $\mathrm{bw}(\varphi, G) - 1$ vertices between u and w in φ; otherwise, the edge $e = (u, w)$ would exceed the bandwidth of φ.

Since every vertex is incident to at most $\Delta(G)$ edges the edge e is crossed by at most $\Delta(G) \cdot (\mathrm{bw}(\varphi, G) - 1)$ other edges, and we have that $\mathrm{lcr}^{\uparrow}(\varphi, G) \leq \Delta(G) \cdot (\mathrm{bw}(\varphi, G) - 1)$. ∎

Now, that we have introduced the crucial parameters of this chapter and the relation under each other, we start by constructing an embedding of the Cartesian product of two paths $P_1 \square P_2$, which local crossing number depends only of a given topological ordering of one input path. For this we will use the so called canonical embedding that was introduced in the end of Section 3.2.1. The properties of the canonical embedding depend on the chosen embedding of the input graphs. For the path we choose a x-unique embedding to avoid unnecessary P-crossings. For the graph G we define an embedding based on an ordering in the following way.

Given a directed graph G and a topological ordering φ of G, we define an embedding $\Gamma(\varphi)$ of G by placing each vertex $v \in V(G)$ at the coordinate $(0, \varphi(v))$ and embedding all edges to the right side of the vertices. We say that a vertex v *lies between* two vertices u and w if $\varphi(u) < \varphi(v) < \varphi(w)$. Using this definition, every topological ordering of G yields a unique corresponding embedding of the graph.

There are important connections between the parameters of the topological ordering φ discussed above and the embedding $\Gamma(\varphi)$, which will be relevant later in this section:

i The number of vertices $v \in V(G)$ that lie between two adjacent vertices u, w with $(u, w) \in E(G)$ — that is, vertices for which $\varphi(u) < \varphi(v) < \varphi(w)$ — equals the length of uw minus 1 and this is bounded by $bw(\varphi, G) - 1$.

ii The set of edges that *nest* a vertex v, meaning v lies strictly between the endpoints of the edge, can be described as $\{(u, w) \in E(G) \mid \varphi(u) < \varphi(v) < \varphi(w)\}$. Comparing this with the definition of the cutwidth, it is clear that the cardinality of this set is bounded by $cw(\varphi, G)$.

iii The embedding $\Gamma(\varphi)$ is upward because φ is a topological ordering.

iv Since the construction of $\Gamma(\varphi)$ is identical to the construction of the embedding used to define $lcr^{\uparrow}(\varphi)$, except for a mirroring along the bisector of the first quadrant's angle, it follows that $lcr^{\uparrow}(\Gamma(\varphi)) = lcr^{\uparrow}(\varphi, G)$.

In particular, the relative positioning of edges and vertices of the embedding $\Gamma(\varphi)$ can be expressed via the parameters of the ordering. With these observations we can discuss all the crossings that appear in the canonical $(\Gamma(\varphi), \Pi_h)$-embedding of the Cartesian product $G \square P$ for a topological ordering φ of G and a x-unique embedding of the orientated path P. We start by analyzing the crossings of G- and P-edges separately and derive from both result a first improved upper bound that is refined for the case that G is also a path, afterward.

We begin by analyzing the crossings of the G-edges.

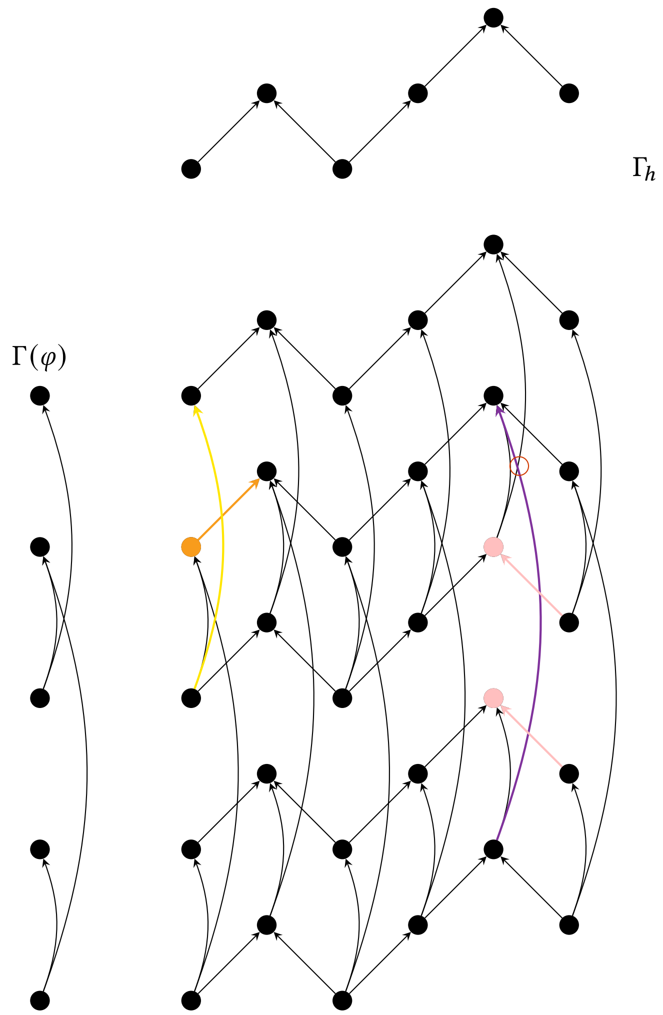

Figure 3.16: This figure illustrates the canonical $(\Gamma(\varphi), \Gamma_h)$-embedding, where $\Gamma(\varphi)$ is the vertical embedding shown on the left, and Γ_h is the horizontal embedding shown at the top. For this example, $\Gamma(\varphi)$ yields the following parameters: $lcr^{\uparrow}(\varphi) = 1$, $bw(\varphi) = 3$, and $cw(\varphi) = 3$. The crossing analysis of the P_v-edges is highlighted in violet. The chosen P_v-edge e in the embedding of the Cartesian product is crossed by every edge whose left endpoint is nested by e (these are marked in magenta), as well as by the crossings that already occur in $\Gamma(\varphi)$ (circled in pink). The crossing analysis of the P_h-edges is indicated in orange. Here, the chosen edge is crossed by every P_v-edge that nests its left endpoint; these edges are marked in yellow. Using the formula from Corollary 3.15, we find that the upward local crossing number is at most 3. By explicitly counting the crossings in the figure, we confirm that this bound is tight.

Lemma 3.12: *Let P be and orientated path and G a directed acyclic graph, let φ be a topological ordering of G and Γ_h a x-unique embedding of P. Then, in the canonical $(\Gamma(\varphi), \Gamma_h)$-embedding no G-edge is crossed more than $bw(\varphi) - 1 + lcr^{\uparrow}(\varphi)$ times.*

The general idea of the embedding that leads to this bound and the analysis of potential crossings is illustrated in Figure 3.16.

Proof. To establish the bound, we count the maximum possible number of crossings for an arbitrary G-edge $e = (u, w)$. Recall, that the canonical embedding ensures that G-copies do not cross other G-copies. The only possible crossings occur either within the G-copy of e, where e can cross other G-edges, or with P-edges whose left endpoint lies in the same G-copy as e.

The crossings within a G-copy are bounded by $lcr^{\uparrow}(\Gamma(\varphi)) = lcr^{\uparrow}(\varphi)$.

Furthermore, for e to cross a P-edge, the left endpoint of that P-edge must lie between u and w. By observation (i) and due to the fact that in a path every vertex is the left endpoint of at most one edge, this can happen for at most $bw(\varphi) - 1$ such P-edges.

In total, e can therefore be crossed at most $(bw(\varphi) - 1) + lcr^{\uparrow}(\varphi)$ times. ∎

Note that, in every G-copy (except for the copy most on the right), the longest edge is crossed at least $bw(\varphi) - 1$ times. If this longest edge is also the edge with the most crossings in $\Gamma(\varphi)$, then this bound is tight for the G-edges.

Next, we analyze the crossings of the P-edges.

Lemma 3.13: *Let P be and orientated path and G a directed graph, let φ be a topological ordering of G and Γ_h a x-unique embedding of P. Then, in the canonical $(\Gamma(\varphi), \Gamma_h)$ no P-edge is crossed more than $cw(\varphi)$ times.*

Proof. Analogous to the proof of Lemma 3.12, we count the maximum number of crossings of an arbitrary P-edge $e' = (v, x)$. The only possible crossings occur within the P-copy of e' with other P-edges or with G-edges that lie in the same G-copy as the left endpoint of e'. We begin with the crossings other P-edges. By Lemma 3.1, the embedding of every P-copy is upward planar; so there are no other crossings between the P-edges within a copy. Therefore, the only possible crossings are with G-edges. For e' to cross a G-edge e, the left endpoint of e' must be nested between the endpoints of e. According to observation (ii), there are at most $cw(\varphi)$ edges that satisfy this condition. Thus, e' is crossed at most $cw(\varphi)$ times. ∎

Similar to before, we can also analyze in which cases the boundary is tight. For this, we call a vertex $v \in V(G)$ with

$$|\{\, uw \in E(G) \mid \varphi(u) < \varphi(v) \leq \varphi(w) \,\}| = cw(\varphi)$$

a *cutwidth-certifying vertex.* That is, when the gap between v and its predecessor certifies the cutwidth of the embedding. By comparing this property with observation (ii), we conclude that a cutwidth-certifying vertex v must be nested between exactly $cw(\varphi) - d_{in}(v)$ vertices in $\Gamma(\varphi)$. Consequently, any P-edge whose left endpoint is such a vertex v is crossed precisely $cw(\varphi) - d_{in}(v)$ times. We further observe that a vertex with $d_{in}(v) = 0$ can never be a cutwidth-certifying vertex. Moreover, since it is possible that $d_{in}(v) < \Delta_{in}(G)$, a tight upper bound can only be formulated under the assumption that all vertices with $d_{in}(v) > 0$ have the same in-degree—for example, when G is a path. In particular, if G is an orientated path, the bound for the number of crossings of P-edges is tight and equals $cw(\varphi) - 1$.

To conclude, from Lemma 3.12 and Lemma 3.13, any edge in the canonical $(\Gamma(\varphi), \Gamma_h)$-embedding is crossed at most

$$\max\left(bw(\varphi) + lcr^{\uparrow}(\varphi) - 1,\ cw(\varphi)\right) \tag{3.1}$$

times.

Considering Lemma 3.10 and Lemma 3.11 and the fact that $bw(G) \leq bw(\varphi)$ for all topological orderings φ we conclude the following corollary.

Corollary 3.14: *There exists an embedding Γ_C of the Cartesian product of a directed graph G and an orientated path P, with $lcr^{\uparrow}(\Gamma_c) \in O(\Delta(G) \cdot bw(G))$*

To find a more specific and better bound, we have to find a topological ordering that minimize the maximum in Equation (3.1). Furthermore, if G is a path as well, we may switch the roles of G and P and choose a topological ordering of P that minimizes the value even further. This leads to the following conclusion.

Corollary 3.15: *There exists an embedding of the Cartesian product of two orientated paths P_1 and P_2 that is p^*-upward planar, where*

$$p^* := \min\left(p^*(P_1),\ p^*(P_2)\right)$$

and

$$p^*(P_i) := \min_{\varphi \in \Phi(P_i)} \max\left(bw(\varphi) + lcr^{\uparrow}(\varphi) - 1,\ cw(\varphi)\right)$$

for $i \in \{1, 2\}$.

Instead of expressing the bound in terms of the cutwidth and bandwidth of the path, we can formulate it now based on structural characteristics of the orientated path itself.

Suppose we label the vertices of a path according to their order along the underlying undirected path. This naturally induces two directions: one in which the label increases along an edge, and one in which it decreases. A sequence of consecutive edges that are all orientated in the same direction is referred to as a *monotone* subpath. A subpath is *maximal monotone* if it cannot be extended further by including adjacent edges that follow the same direction. Depending on the orientation, a monotone subpath is called *increasing* or *decreasing*.

Let $\ell_{\uparrow}$ denote the length of the longest increasing subpath, and $\ell_{\downarrow}$ the length of the longest decreasing subpath. By appropriately labeling the vertices of the path, we can always ensure that one of the longest maximal monotone subpaths is increasing.

Figure 3.17 illustrates these relevant characteristics and will be used throughout this section to demonstrate the construction of an ordering based on these different structural properties.

Using the formula from Corollary 3.15, we can derive a more refined upper bound for the upward local crossing number of the Cartesian product of two orientated paths. This bound depends on the number of maximal monotone subpaths and the length of the longest monotone decreasing subpath.

Lemma 3.16: *For an orientated path P_1 on n vertices with k maximal monotone subpaths and an arbitrarily orientated path P_2 the upward local crossing number of their Cartesian product is bounded by:*

$$lcr^{\uparrow}(P_1 \square P_2) \leq \begin{cases} 3(k-1) & k > 2 \\ 4 & k = 2 \end{cases}.$$

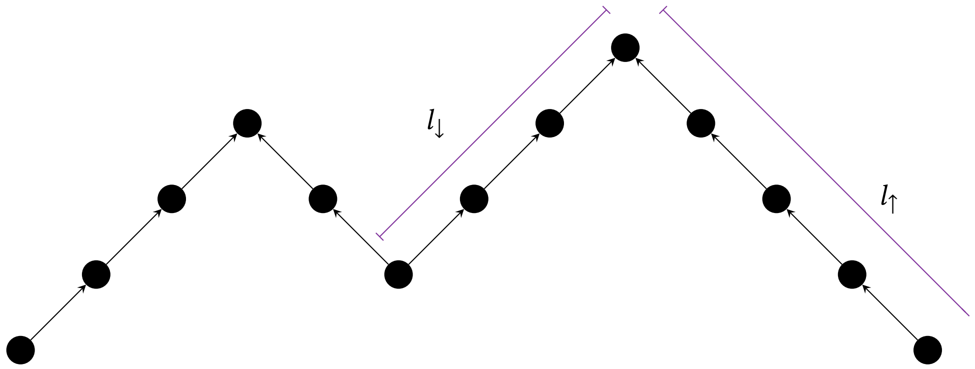

Figure 3.17: An orientated path on 13 vertices with 4 maximal monotone subpaths. The longest maximal monotone subpath is the one embedded most on the right, with $\ell_\uparrow = 4$. If we label the vertices from right to left, this subpath is increasing. Then longest monotone decreasing subpath has length $\ell_\downarrow = 3$.

Note that for $k = 1$, P_1 is a monotone path and we have already shown that the embedding of the Cartesian product with any other path is upward planar.

Proof. We construct an topological ordering φ_1 of P_1 such that $bw(\varphi_1, P_1) \leq k$ and use this to derive the desired bound with the help of the formula from Corollary 3.15 in combination with Lemma 3.10 and Lemma 3.11 which bounds the cutwidth and upward local crossing number by the bandwidth. To construct φ_1, we first create a horizontal embedding of P_1 and then label the vertices according to their position along the x-axis. This is illustrated in Figure 3.18, based on the path from Figure 3.17. After the construction we show that φ_1 fulfills all the wanted properties.

To construct the embedding, we divide the x-axis into disjoint segments, which we refer to as *buckets*. Each bucket contains k distinct horizontal positions or *slots*. We label the slots in every bucket from left to right using the labels $\{0, 1, \ldots, k-1\}$.

Next, we traverse the underlying undirected path of P_1, processing it one maximal monotone subpath at a time, from left to right. We assign each of these k subpaths a unique identifier from the set $\{0, 1, \ldots, k-1\}$, according to their position in the sequence of the subpaths.

We begin with the first subpath, which is assigned the number 0. The vertices of this subpath are placed into consecutive buckets such that each vertex occupies the slot labeled 0. The direction of the edges between these vertices is left to right, ensuring consistency with an upward orientation.

For the second subpath (assigned the label 1), we place its next vertex in the next available slot labeled 1, directly above or below the previous subpath's last vertex—depending on the edge orientation. Note that the first vertex of the second subpath was already embedded as part of the first subpath - therefore the *next* vertex is the second vertex of the path. We then embed the remaining vertices of this subpath into successive buckets, always placing them in the slot labeled 1, and maintaining a left-to-right edge direction.

We repeat this embedding process for all remaining maximal monotone subpaths, always embedding the vertices into slots with the respective identifier of the subpath. After embedding all vertices, we define the ordering φ_1 by scanning the embedding from left to right and assigning the vertex labels accordingly.

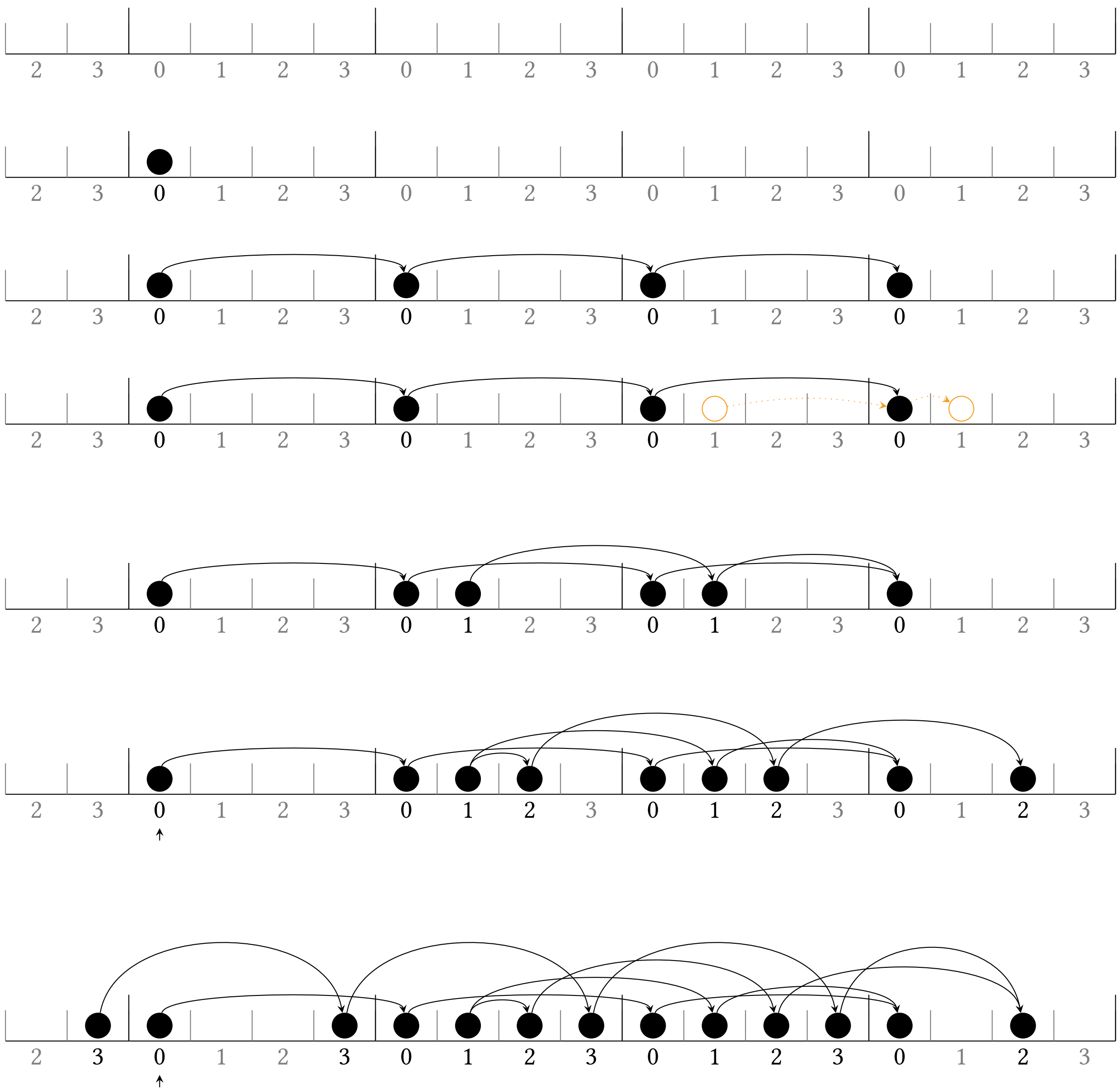

Figure 3.18: This illustrates the construction process in the proof of Lemma 3.16. In the first step we divide the x-axis into buckets with $k = 4$ spots each. After that, we place the first subpath in the spot “0” of consecutive buckets. Dependent on the edge orientation we place the next vertex in a slot “1” below or above the last vertex of our previous path. In the illustration it is easy to see, that this slot has always a distance less than $k - 1$. The rest of the second subpath is inserted in slots with label “1”. The other subpath are embedded the same way in slots with increasing label. The final result is presented in the last row: The vertex embedded most on the left in Figure 3.17 is marked by an arrow. We see, that the vertices of one subpath except for first vertex are always equidistant. We receive a topological ordering by scanning the vertex order from left to right.

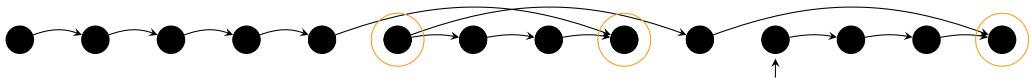

Figure 3.19: The ordering of the path shown in Figure 3.17 based on $\ell_\downarrow$, as described in the proof of Lemma 3.17. The vertex embedded furthest to the left in Figure 3.17 is marked with an arrow.

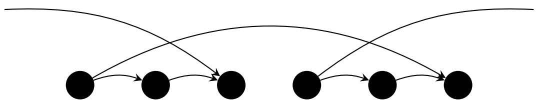

Figure 3.20: A section of a possible path ordering according to Figure 3.19. This occurs when two decreasing subpaths are connected by a single increasing edge, which then spans both decreasing subpaths.

Now we show that φ_1 is a topological ordering with $bw(\varphi_1, P_1) \leq k$. Since every edge is directed from left to right and we assign the vertex labels for the ordering by scanning from left to right, φ_1 is indeed a topological ordering.

Furthermore, recall that the length of an edge in the ordering corresponds to the number of vertices (or positions) between its endpoints in the initial embedding. Due to our construction, except for the first vertex of a monotone subpath, all vertices of the same subpath are placed in spots with the same label across adjacent buckets. As a result, there are exactly $k-1$ spots between any two such adjacent vertices along the x-axis, leading to a edge length of at most k.

The length of the edge between the first and second vertex of a maximal monotone subpath can differ. The second vertex of the subpath with identifier j is placed in a spot labeled j, either above or below the previous subpath's last vertex (which is also the first vertex of the subpath j), which was placed in a spot labeled $j-1$. Since these labeled spots are within the same bucket or adjacent buckets, the distance between label $j-1$ and label j is at most $k-1$, regardless of whether it is positioned above or below. Thus, the edge connecting these two vertices has length at most $k-1$. Consequently, the number of positions (and thus vertices) between the endpoints of any edge is at most $k-1$. This implies that the bandwidth of the ordering is at most k, i.e., $bw(\varphi_1, P_1) \leq k$.

By applying Lemma 3.10 and Lemma 3.11, we obtain the following bound:

$$p^*(P_1) \leq \max(bw(\varphi) + lcr^\uparrow(\varphi) - 1, cw(\varphi)) \leq \max(k + 2(k-1) - 1, 2k) = \max(3(k-1), 2k).$$

With this result and Corollary 3.15, the claim follows immediately. ∎

Next, we define a bound dependent on the length of the longest maximal monotone decreasing subpath.

Lemma 3.17: *For an orientated path P_1 with n vertices and a longest maximal monotone decreasing subpath of length $\ell_\downarrow$, and for an arbitrary orientated path P_2, the upward local crossing number of their Cartesian product satisfies:*

$$lcr^\uparrow(P_1 \square P_2) \leq 2l_\downarrow + 3$$

Proof. Let P_1 be a path whose longest maximal monotone decreasing subpath has length $\ell_\downarrow$. We denote this subpath by P_l. Similar to the proof of Lemma 3.16, we begin by constructing a topological ordering φ_1 of P_1, this time based on the parameter $\ell_\downarrow$.

We show that φ_1 is a valid topological ordering and that its bandwidth, cutwidth, and upward local crossing number are each bounded by either $\ell_\downarrow$ or a constant. Using these bounds, we apply Corollary 3.15 to derive the desired result.

The construction of this ordering for the path in Figure 3.17 is illustrated in Figure 3.19.

Now, suppose vertex $i \in \{1, \ldots, n-1\}$ has a neighbor $i-1$ already placed in the ordering. There are two possibilities for the direction of the edge e between i and $i-1$: If $e = (i-1, i)$, then we insert vertex i at the rightmost position in the ordering. In particular, this means placing i to the right of $i-1$. Otherwise, if $e = (i, i-1)$, then we insert i directly to the left of $i-1$.

Due to the construction process φ_1 is a topological embedding.

Before analyzing the parameters of the ordering, we highlight an important observation to understand its structure: With this construction, any increasing edge adjacent to a decreasing subpath always spans that subpath. This is because the vertices of the decreasing subpath are inserted between the endpoints of the increasing edge, or the increasing edge spans the entire subpath to ensure that the next vertex is assigned the rightmost label. All other edges have length 1.

A single edge can be adjacent to at most two decreasing subpaths. In such a case, the edge spans both subpaths, as illustrated in Figure 3.20.

With these insights, we analyze the **bandwidth** first. Since an edge can span at most two decreasing subpaths, and each subpath contains at most $\ell_\downarrow + 1$ vertices, the bandwidth is bounded by:

$$bw(\varphi_1, P_1) \leq 2(\ell_\downarrow + 1)$$

Next, we consider the **cutwidth**. Because only decreasing subpaths are spanned by other edges, cuts at vertices in increasing subpaths are only crossed by the incident edges. A cut within a decreasing subpath can be crossed by the edge within the subpath itself and up to two increasing edges that span the entire subpath. Thus, we conclude:

$$cw(\varphi_1, P_1) \leq 3$$

Lastly, we analyze the **upward local crossing number**. Crossings can only occur between edges that span the same decreasing subpath. Since at most two edges can span a given subpath, an edge that spans one subpath can be crossed at most once. An edge that spans two subpaths can be crossed by at most two other edges. Therefore:

$$lcr^{\uparrow}(\varphi_1) \leq 2$$

Now we can use these bounds and the formula from Corollary 3.15. In conclusion, for this embedding φ_1, it holds that:

$$\max(bw(\varphi_1) + lcr^{\uparrow}(\varphi_1) - 1, cw(\varphi_1)) \leq \max(2(\ell_\downarrow + 1) + 2 - 1, 3) = 2\ell_\downarrow + 3$$

∎

Using Corollary 3.15 and Lemma 3.10, we establish an upper bound on the upward local crossing number of the Cartesian product of two arbitrarily orientated paths P_1 and P_2. Given a topological ordering φ_1 of P_1, it holds that $\mathrm{lcr}^{\uparrow}(P_1 \square P_2) \leq \max(\mathrm{bw}(\varphi_1) + \mathrm{lcr}^{\uparrow}(\varphi_1) - 1,\ cw(\varphi_1))$.

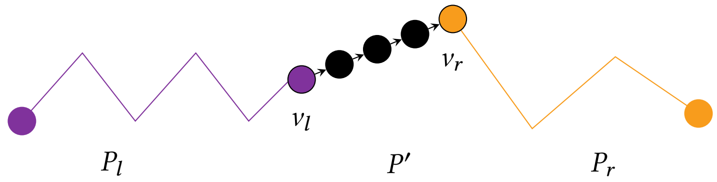

Figure 3.21: This figure illustrates the structure of a path P containing $p+1$ monotone subpaths with length greater than $\sqrt{n}$, as introduced in the proof of Lemma 3.19. The subpath P' highlighted in black is one such maximal monotone subpath, with endpoints labeled v_l and v_r. The vertex v_l denotes the start vertex of P'. The subpath P_l, here, located to the left of P', is highlighted in orange, while P_r, located to the right of P', is shown in violet. Note that v_l belongs to both P_l and P', and similarly, v_r belongs to both P_r and P'.

Applying the bounds from Lemma 3.10 and Lemma 3.11, we get $\text{lcr}^{\uparrow}(P_1 \,\square\, P_2) \leq \max(3 \cdot \text{bw}(\varphi_1),\ 2 \cdot \text{bw}(\varphi_1)) = 3 \cdot \text{bw}(\varphi_1)$. Since we can choose φ_1 such that $\text{bw}(\varphi_1) = \text{bw}(P_1)$, it follows that $\text{lcr}^{\uparrow}(P_1 \,\square\, P_2) \leq 3 \cdot \text{bw}(P_1)$. We argue analogously for a topological ordering φ_2 of P_2 and combine both insights in the following corollary.

Corollary 3.18: *For all orientated paths P_1, P_2 it holds that* $\text{lcr}^{\uparrow}(P_1 \square P_2) \leq 3 \cdot \min(\text{bw}(P_1), \text{bw}(P_2))$.

Therefore, by bounding the bandwidth of orientated paths, we obtain a general upper bound for the upward local crossing number of their Cartesian product.

Lemma 3.19: *For all orientated paths P on n vertices it holds that* $\text{bw}(P) \leq 4\sqrt{n}$.

Proof. Let P be an orientated path on n vertices. In order to show this claim we prove that $\text{bw}(P) \leq 2 \cdot (\sqrt{n} + p)$ with p being the number of maximal monotone subpaths with length at least $\sqrt{n}$. We proceed by induction on p. For the base case $p = 0$, the longest monotone subpath has length smaller than $\sqrt{n}$. Thus, by Lemma 3.17 it holds that $\text{bw}(P) \leq 2 \cdot \sqrt{n}$. Assume that the inequality holds for all paths with p maximal monotone subpaths with length at least $\sqrt{n}$ for some $p \in \mathbb{N}_0$ and let P be a path with $p+1$ maximal monotone subpaths with length at least $\sqrt{n}$. Then we construct a topological ordering φ of P with $\text{bw}(\varphi, P) \leq 2 \cdot (\sqrt{n} + p + 1)$.

Let P' be a monotone subpath of P with length at least $\sqrt{n}$. Denote the endpoints of P' by v_l and v_r, where the edges of P' are directed from v_l to v_r. Define P_l as the connected component of the graph $P - (P' - \{v_l, v_r\})$ that contains v_l. Analogously, let P_r be the component that contains v_r. Thus, P_l and P_r represent the two subpaths on either side of P', as illustrated in Figure 3.21.

Observe that both P_l and P_r contain at most p monotone subpaths of length at least $\sqrt{n}$. So we may assume by induction that there exist topological orderings φ_l and φ_r of P_l and P_r, respectively, such that $\text{bw}(\varphi_k, P_k) \leq 2 \cdot (\sqrt{n} + p)$ for $k \in \{l, r\}$.

We now construct a topological ordering φ of P based on φ_l and φ_r. This construction is illustrated in Figure 3.22. First, we concatenate φ_l and φ_r into an auxiliary ordering, denoted by φ_{l+r}, such that all vertices of P_r receive a higher label than all vertices of P_l. That is, for all $v \in V(P_l)$ and $v' \in V(P_r)$ it holds that $\varphi_{l+r}(v) < \varphi_{l+r}(v')$.

Define v_l^* as the vertex in P_l with the highest label under φ_{l+r}, i.e., $\varphi_{l+r}(v_l^*) = \max\{\varphi_{l+r}(v) \mid v \in V(P_l)\}$, and v_r^* as the vertex in P_r with the lowest label under φ_{l+r}, i.e., $\varphi_{l+r}(v_r^*) = \min\{\varphi_{l+r}(v') \mid v' \in V(P_r)\}$. Note, that v_l^* and v_r^* have consecutive labels under φ_{l+r}.

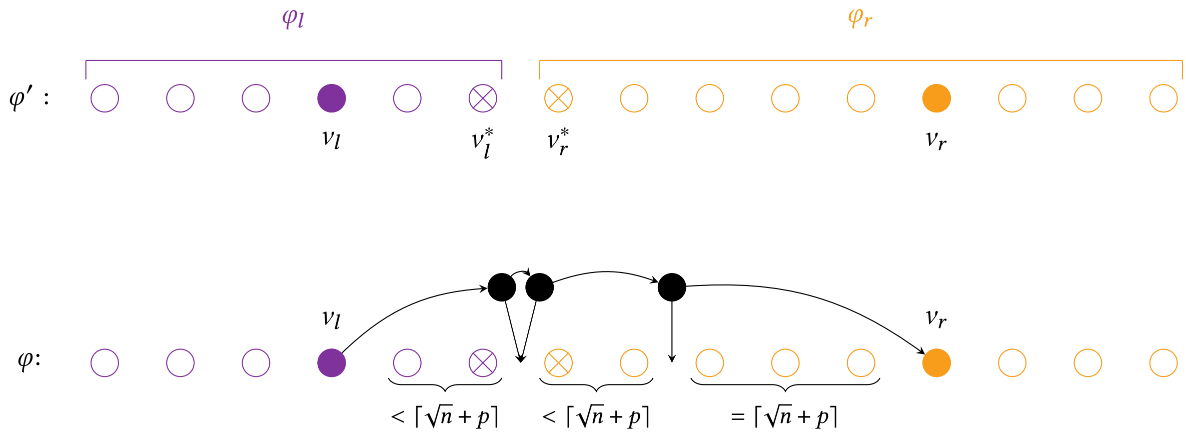

Figure 3.22: This illustrates the construction process of φ under the assumption that $\lceil\sqrt{n}+p\rceil$ = 3. The first steps shows the concatenation of φ_l and φ_r, the second the insertion of the internal vertices of P'. The characteristic vertices v_l^* and v_r^* are marked by a cross.

Next, we insert the internal vertices of P' into φ_{l+r} to obtain a total ordering of P. Specifically, we place the vertices such that between any two adjacent vertices $u, w \in V(P')$ with $(u, w) \in E(P')$, there are at most $\lceil\sqrt{n}+p\rceil$ vertices between them. Additionally, between any two adjacent vertices x, y in P_l or P_r, there are only a bounded number of vertices of P' inserted.

We define this embedding formally by inserting the first $\frac{|\varphi_l(v_l)-\varphi_l(v_l*)|}{\lceil\sqrt{n}+p\rceil}$ of P' between v_l and v_l*, such that there are exactly $\lceil\sqrt{n}+p\rceil$ vertices between two adjacent vertices of P'. Recall, that v_l is also a vertex of P'. Analogously, we insert the last $\frac{|\varphi_r(v_r)-\varphi_r(v_r*)|}{\lceil\sqrt{n}+p\rceil}$ of P' between v_r^* and v_r, such that there are also exactly $\lceil\sqrt{n}+p\rceil$ vertices between two adjacent vertices of P'. All the other vertices are inserted consecutively between v_l^* and v_r^*. The resulting order ist denoted by φ.

We show that φ is a topological ordering of P and that $\mathrm{bw}(\varphi, P) \leq 2 \cdot (\sqrt{n}+p+1)$ by showing that the length of every edge with respect to φ is at most $2 \cdot (\sqrt{n}+p+1)$.

First, we verify that φ is a valid ordering of P. Assume, for contradiction, that $\frac{|\varphi_l(v_l)-\varphi_l(v_l*)|}{\lceil\sqrt{n}+p\rceil} + \frac{|\varphi_r(v_r)-\varphi_r(v_r*)|}{\lceil\sqrt{n}+p\rceil} > |V(P')|$. However, since P' contains at least $\sqrt{n}$ vertices, this would mean that there are more than $\sqrt{n} \cdot \lceil\sqrt{n}+p\rceil \geq n$ vertices between v_l and v_r, which contradicts the fact that P contains only n vertices in total.

Moreover, note that the restriction of φ to the vertices of P_l, P_r, or P' coincides with the topological orderings φ_l, φ_r and the unique topological ordering of the monotone subpath P', respectively (particularly since $\varphi(v_l) < \varphi(v_r)$). Therefore, φ is indeed a topological ordering of P.

Before analyzing the lengths of various edges, we make the following observation: for every $k \in \mathbb{N}$, if two vertices $u, w \in V(P_l)$ have a distance of at most $k \cdot \lceil\sqrt{n}+p\rceil$ with respect to the auxiliary ordering φ_{l+r}, then by the construction of φ, at most k vertices from P' are inserted between u and w in φ. An analogous statement holds for vertices in P_r.

Now, we analyze the length of edges with respect to the ordering φ. Recall that the length of an edge is defined as the absolute difference between the labels of its endpoints, and the bandwidth of an ordering is the maximum length over all edges. For any edge $e \in E(P')$, the construction ensures that the labels of its endpoints differ by at most $\lceil \sqrt{n} + p \rceil$, since at most this many vertices are inserted between any two adjacent vertices in P'.

Consider an edge $e = (u, w) \in E(P_l)$. The length of e with respect to φ depends on its length under φ_l, plus the number of vertices from P' that were inserted between u and w during the construction of φ. Since we assumed that $\text{bw}(\varphi_l, P_l) \leq 2(\sqrt{n} + p)$, the previously established observation implies that at most two vertices from P' were inserted between u and w.

Therefore, we obtain the following bound:

$$|\varphi(u) - \varphi(w)| \leq |\varphi_l(u) - \varphi_l(w)| + 2 \leq 2(\sqrt{n} + p) + 2 = 2(\sqrt{n} + p + 1).$$

The second inequality holds because we assumed that φ_l satisfies $\text{bw}(\varphi_l, P_l) \leq 2(\sqrt{n} + p)$.

A similar argument applies to every edge $e \in E(P_r)$. Since $E(P) = E(P_l) \cup E(P') \cup E(P_r)$, we conclude that the length of every edge in P is at most $2(\sqrt{n} + p + 1)$, and hence $\text{bw}(\varphi, P) \leq 2(\sqrt{n} + p + 1)$. This concludes the induction and we have that $\text{bw}(P) \leq 2 \cdot (\sqrt{n} + p)$.

Finally, since $p \leq \sqrt{n}$, it follows that $\text{bw}(P) \leq 4\sqrt{n}$. ∎

By combining Lemma 3.19 and Corollary 3.18, we arrive at the following result:

Corollary 3.20: *Let P_n and P_m be arbitrary orientated paths. Then, the Cartesian product $P_n \square P_m$ is k-upward planar with $k \in \mathcal{O}(\sqrt{\min(n, m)})$.*

3.2.3 Upper Bound for Cartesian Products of Upward k-Planar Graphs

In this section we derive an improved upper bound for the Cartesian product of two directed, acyclic graphs by using the in Section 3.2.1 introduced canonical embedding. Before extending our own results onto the Cartesian product of directed graphs, we first establish an upper bound that follows directly from previously published work.

Theorem 3.21 ([Ang+25])**:** *For every directed acyclic graph it holds that*

$$\text{lcr}^{\uparrow}(G) \leq \text{bw}(G)^2,$$

.

If we bound the bandwidth of the Cartesian product dependent on the input graph, we can derive an upper bound immediately. For this purpose, we rely on a result mentioned by Kojima and Ando [KA02] and introduced by Chvátalová, Dewdney, Gibbs, and Korfhage [CDGK75].

Theorem 3.22: *For two graphs G and H it holds that*

$$\text{bw}(G \square H) \leq \min\left(\text{bw}(H) \cdot |V(G)|,\ \text{bw}(G) \cdot |V(H)|\right)$$

.

Proof. We illustrate the idea of the proof. First we show that $\mathrm{bw}(G\square H) \leq \mathrm{bw}(H)\cdot|V(G)|$. Take an ordering φ_H that minimzises the bandwidth for the graph H. We substitute every vertex in the ordering by a vertex set of G. With this, we obtain an ordering of Cartesian product $G \square H$ where a vertex $(g, h) \in V(G \square H), g \in V(G), h \in V(H)$ inherits the label of the vertex g in that copy of G that replaced h in the ordering φ_H. Then every edge in a G-copy as length of at most $|V(G)|$ and every edge in a H-copy has length of $\mathrm{bw}(\varphi_H) \cdot |V(G)| = \mathrm{bw}(H) \cdot |V(G)|$. We switch the roles of G and H and take the minimum of both bounds, which leads to the result. ∎

Combining Theorem 3.21 and Theorem 3.22 we conclude the following corollary.

Corollary 3.23: *The upward local crossing number of the Cartesian product of two directed graphs G and H can be bounded by*

$$\mathrm{lcr}^{\uparrow}(G \square H) \leq \min\left(\mathrm{bw}(H)^2 \cdot |V(G)|^2,\ \mathrm{bw}(G)^2 \cdot |V(H)|^2\right).$$

We now construct a more specific upper bound based on our previous results. To this end, we define special topological orderings that are induced by a given upward embedding. For an upward embedding $\Gamma(G)$ of a graph G, we define the topological ordering $\varphi_{(\Gamma(G),x)}$ as the ordering obtained by altering the embedding in a way that every vertex has a unique x-coordinate such that the resulting embedding is still equivalent to $\Gamma(G)$ and then scanning the vertices of $\Gamma(G)$ from left to right. Analogously, we define the topological ordering $\varphi_{(\Gamma(G),y)}$ as the ordering obtained by altering the embedding such that every vertex has a unique y-coordinate and then scanning the vertices of $\Gamma(H)$ from bottom to top.

With these definitions, we can formulate the following statement.

Theorem 3.24: *Let G_h and G_v be two directed graphs. Suppose G_h admits an upward k_h-planar embedding $\Gamma_h := \Gamma(G_h)$ and G_v an upward k_v-planar embedding $\Gamma_v := \Gamma(G_v)$. Define $\varphi_h := \varphi_{(\Gamma(G_h),x)}$ and $\varphi_v := \varphi_{(\Gamma(G_v),y)}$. Then, the upward local crossing number k' of the Cartesian product $G_h \square G_v$ is bounded by*

$$k' \leq \max\left(\mathrm{bw}(\varphi_h) \cdot \mathrm{cw}(\varphi_v) + k_h,\ \mathrm{bw}(\varphi_v) \cdot \mathrm{cw}(\varphi_h) + k_v\right).$$

The proof strategy closely parallels the reasoning applied in Corollary 3.14. In particular, the construction of the embedding and the subsequent analysis follow the same structural principles. Figure 3.23 highlights the central ideas underlying this argument.

Proof. We show that the canonical (Γ_h, Γ_v)-embedding of the Cartesian product already yields the stated bound. To this end, we estimate the maximum number of crossings of a G_v-edge and, analogously, of a G_h-edge.

Consider an arbitrary G_v-edge $e = (u, w)$. Let G' denote the subgraph of the Cartesian product induced by the G_v-copy containing e. Since G' is isomorphic to G_v, we may interpret φ_v as a valid ordering of G'. By construction, the canonical embedding guarantees that edges of G' do not intersect edges of other G_v-copies. Consequently, e can only be crossed either by other G_v-edges within G' or by edges of G_h.

We first analyze the crossings with other G_v-edges inside the same copy. Since $\mathrm{lcr}^{\uparrow}(\Gamma(G_v)) = k_v$, the edge e can be crossed by at most k_v additional G_v-edges.

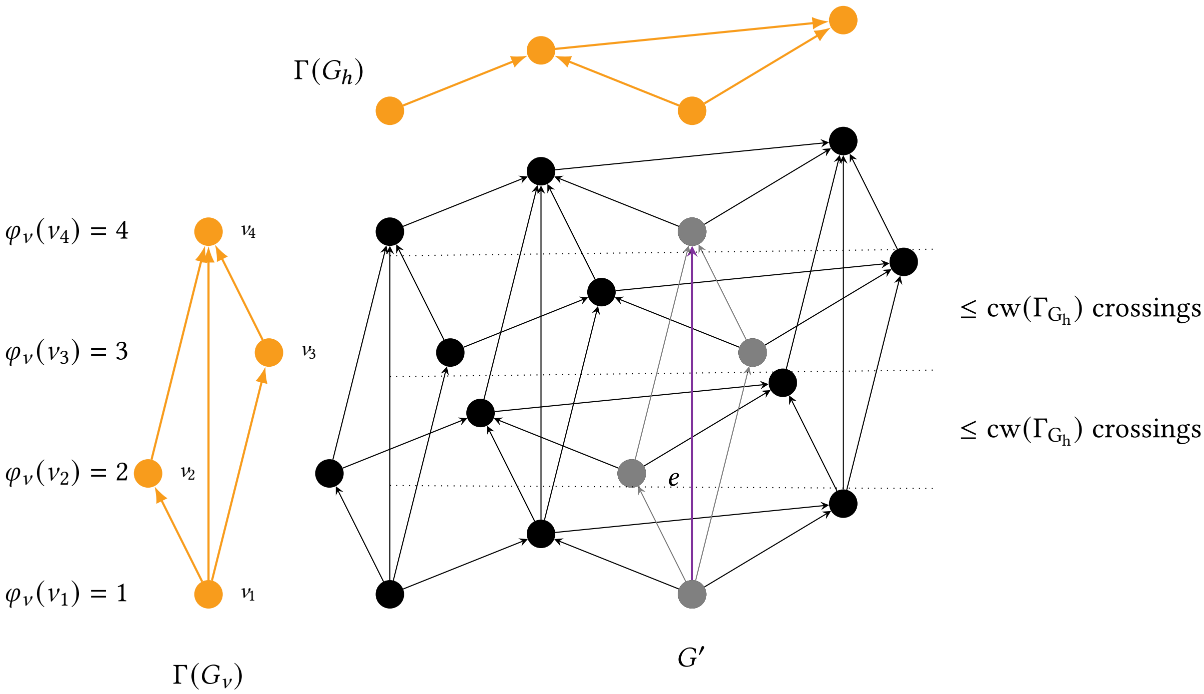

Figure 3.23: The given embeddings $\Gamma(G_h)$ and $\Gamma(G_v)$ are illustrated in orange. Both embeddings are upward planar. For G_v is ordering φ_v is derived. A G_v-egde e in is highlighted in violet in the embedding of the Cartesian product, the copy of G_v that contains is is illustrated in gray and denoted as G'. Observe that e crosses one G_h-copy per vertex hat lie between it is endpoints. In every copy e crosses at most $\mathrm{cw}(\Gamma_{G_v})$ edges. Additionally it crosses edges in the copies of the endpoints, but also at most $\mathrm{cw}(\Gamma_{G_v})$, as illustrated in Figure 3.24.

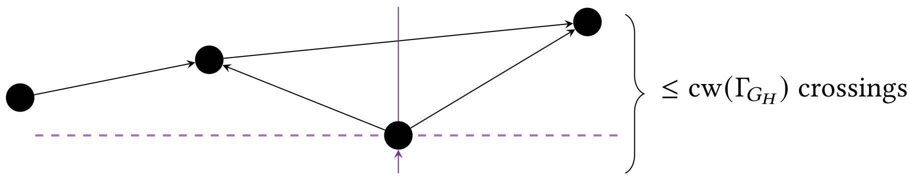

Figure 3.24: Above the dotted line lies the part of the G_h-copy corresponding to the starting vertex of e that can be crossed by e, i.e., the portion embedded above the starting vertex. Below the dotted line lies the part of the G_h-copy corresponding to the endpoint of e that can be crossed by e, i.e., the portion embedded below the endpoint. Observe that these two parts together form a complete Γ_{G_h}-copy. Hence, we may conclude that the total number of crossings of e within the copies corresponding to its endpoints is bounded by $\mathrm{cw}(\Gamma_{G_h})$.

The analysis of the crossings with G_h-edges is more complex. We say that an edge e *crosses a G_h-copy* if there exists a point on the Jordan curve representing e in the embedding that lies below all vertices of the G_h-copy (with respect to the y-coordinate) and another point that lies above all vertices of the copy. If e crosses a G_h-copy, then all G_h-edges intersected by e in this copy define a cut of the graph G_h. By the definition of cutwidth, such a cut contains at most $\mathrm{cw}(\varphi_h)$ edges. Hence, for each G_h-copy that e crosses, it contributes at most $\mathrm{cw}(\varphi_h)$ crossings.

We now estimate how many G_h-copies can be crossed by e. Recall, that every G_h-copy has their own layer on the y-axis, i.e. the projection of the convex hull onto the y-axis does not intersect with the projection of other G_h-copies. For each G_h-copy there exists exactly one vertex in G' that belongs to this copy; we refer to it as the *corresponding vertex*. Naturally, the corresponding vertex resides also within this layer. Since e is upward, the edge e can cross edges in a G_h-copy whenever the corresponding vertex in G' lies between u and w with respect to φ_v, as illustrated in Figure 3.23. The number of such vertices is bounded by $\mathrm{bw}(\varphi_v) - 1$.

In addition to these full copies, e may also cross edges in the copy corresponding to u (those lying above u) and in the copy corresponding to w (those lying below w). Since the embeddings of the copies are identical and u and w coincide in both copies, we can conservatively account for these cases by adding one more copy. This is also illustrated in Figure 3.24. Thus, in total, e may cross at most $\mathrm{bw}(\varphi_v)$ many G_h-copies, each contributing at most $\mathrm{cw}(\varphi_h)$ crossings.

Together with the crossings inside G', this yields the bound; e is crossed by at most $\mathrm{bw}(\varphi_v) \cdot \mathrm{cw}(\varphi_h) + k_v$ edges.

An analogous argument applies to any G_h-edge e', where the roles of the x- and y-axis are swapped. We obtain the bound that every G_h-edge is crossed by at most $\mathrm{bw}(\varphi_h) \cdot \mathrm{cw}(\varphi_v) + k_h$ edges.

Taking the maximum of the two estimates completes the proof. ∎

Considering Lemma 3.10 and Lemma 3.11, and using the fact that $\mathrm{bw}(G) \leq \mathrm{bw}(\varphi)$ for every topological ordering φ of a graph G, we obtain the following corollary.

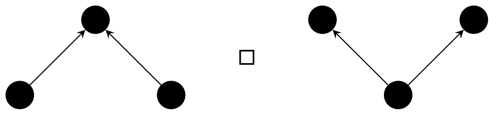

Figure 3.25: A subgraph present in every Cartesian product of two paths where one path has at least one vertex with $d_{\text{in}} = 2$ and the other path has at least one vertex with $d_{\text{out}} = 2$. This subgraph is not upward planar.

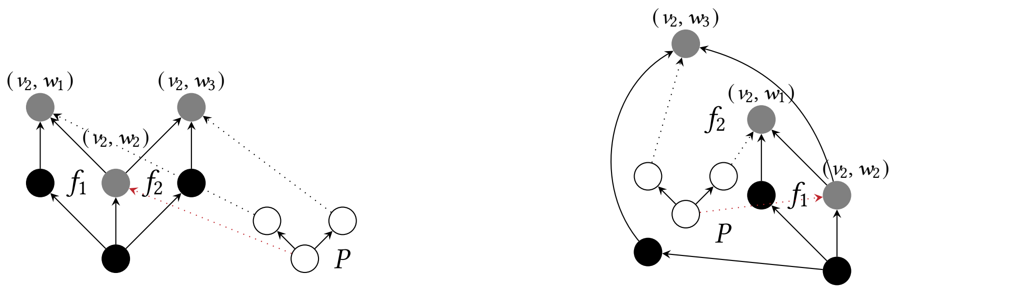

(a) First approach

(b) Second (and third) approach

Figure 3.26: Illustration of the approaches explained in the proof of Theorem 3.26 trying to embed the graph of Figure 3.25 planar. It illustrates that after embedding the two circles C_1, C_2 without crossings there is no way to embed the rest of the Cartesian product – the subgraph P— without crossings. The vertex set V' is illustrated in gray.

Corollary 3.25: *Let G_1 and G_2 be two directed acyclic graphs. Then, there exists an embedding Γ of the Cartesian product of two directed graphs G_1, G_2 such that*

$$\text{lcr}^{\uparrow}(\Gamma) \in O\Big(\max\big(\text{bw}(G_1), \text{bw}(G_2)\big)^3\Big).$$

3.3 Lower Bound for Cartesian Product of Paths

After analyzing an upper bound for the upward local crossing number of Cartesian products of paths, the question we are about to investigate is how complex must the orientation of the two paths be so that no upward planar embedding of their Cartesian product is possible. We show that it is impossible if the Cartesian product contains Figure 3.25 or Figure 3.29 as a subgraph.

Theorem 3.26: *For two orientated paths P_1 and P_2, where P_1 contains at least one vertex with $d_{in} = 2$ and P_2 contains at least one vertex with $d_{out} = 2$, there exists no upward planar embedding of the Cartesian product $P_1 \,\square\, P_2$.*

Proof. We show that the Cartesian product illustrated in Figure 3.25 — which is a subgraph of every Cartesian product of two paths P_1 and P_2 with P_1 having at least one vertex with $d_{in} = 2$ and P_2 having at least one vertex with $d_{out} = 2$ — cannot be embedded upward planar.

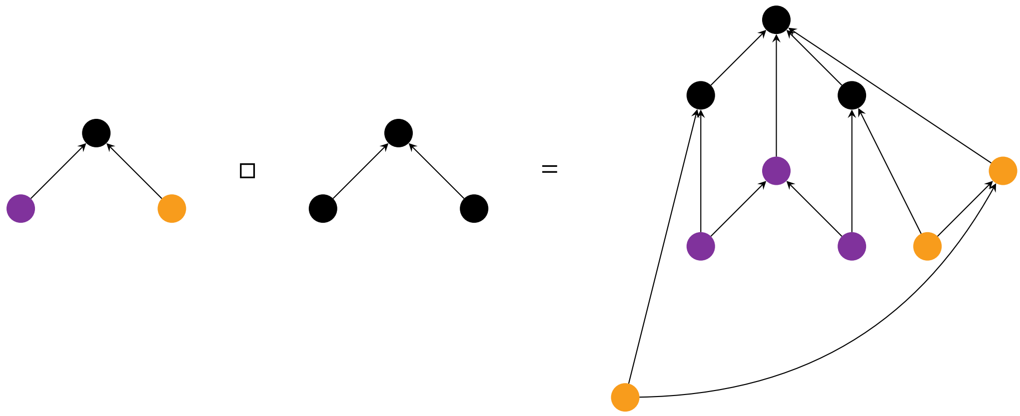

Figure 3.27: Upward planar embedding of the Cartesian product of the graph $G = (\{0, 1, 2\}, \{(0, 1), (2, 1)\}$ with itself.

We denote the vertices of the left input graph in Figure 3.25 by $\{v_1, v_2, v_3\}$ such that $d_{in}(v_2) = 2$, and the vertices of the right input graph by $\{w_1, w_2, w_3\}$ such that $d_{out}(w_2) = 2$. The Cartesian product of these two input graphs has nine vertices $\{v_1, v_2, v_3\} \times \{w_1, w_2, w_3\}$. We attempt to construct an upward planar embedding.

Consider the two cycles in the Cartesian product: C_1 induced by $\{(v_1, w_1), (v_1, w_2), (v_2, w_1), (v_2, w_2)\}$ and C_2 induced by $\{(v_1, w_3), (v_1, w_2), (v_2, w_3), (v_2, w_2)\}$. They share the edge $((v_1, w_2), (v_2, w_2))$. There are only three ways to embed C_1 and C_2 together without crossings in the plane: side-by-side, or one cycle nested inside the other. These configurations are illustrated in Figure 3.26 with f_i being the face that is bounded by C_i for $i \in \{1, 2\}$. Note that the third configuration is essentially the second configuration in Figure 3.26b, but with the roles of C_1 and C_2 swapped.

In each scenario, we must still embed the subgraph P induced by $\{(v_3, w_1), (v_3, w_2), (v_3, w_3)\}$ in order to obtain a full embedding of the Cartesian product. The vertices $V' = \{(v_2, w_1), (v_2, w_2), (v_2, w_3)\}$ each have edges to P.

In the first approach (Figure 3.26a), all of these vertices V' lie on the outer face. There is no other face, on which all of these vertices of V' lie. Thus, P must also be embedded into the outer face. However, (v_2, w_2) can only have incoming edges from the inner faces; otherwise, those edges are not upward. Hence, the configuration in Figure 3.26a does not yield an upward planar embedding.

In the second approach (Figure 3.26b), the vertices V' lie on the inner face f_2. In this case, this face is the only face, on which all of these vertices lie. This forces the subgraph P, which has to be connected with all three vertices from V', to be embedded into f_2 as well. Yet (v_2, w_2) cannot have incoming upward edges from f_2, so the configuration again fails. The same reasoning applies to the third approach.

Therefore, no upward planar embedding exists for this specific Cartesian product, which proves the claim. ∎

Since any path with more than two maximal monotone subpaths necessarily contains a vertex v with $d_{in}(v) = 2$ and a vertex w with $d_{out}(w) = 2$, we have established in particular that the Cartesian product of two paths is not upward planar whenever one path has more than two maximal monotone subpaths and the other has at least two. On the other hand, recall that if one path is monotone, the Cartesian product is upward planar. Thus, the only

(a) $\hat{P}_{\uparrow}$ **(b)** $\hat{P}_{\downarrow}$

Figure 3.28: Definition of two graphs that are needed in Theorem 3.27.

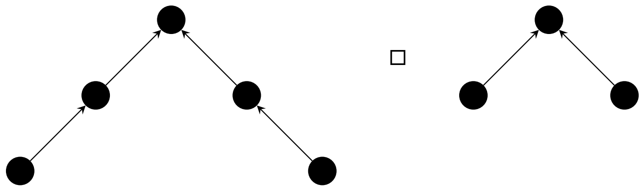

Figure 3.29: Subgraph of every Cartesian product that fulfills the requirements of Theorem 3.27

remaining case to analyze regarding the upward planarity of the Cartesian product of two orientated paths arises when both paths consist of exactly two maximal monotone subpaths and both contain precisely one vertex with $d_{in} = 2$ (or, equivalently, one vertex with $d_{out} = 2$).

Observe that we can embed the product of two paths of length 2, each with exactly one vertex with $d_{in} = 2$, in an upward planar way; see Figure 3.27 for an example.

From this illustration, we can also see that if the subpath on one side of the vertex with $d_{in} = 2$ becomes longer-regardless of whether this occurs in just one path or in both paths — we can still construct an upward planar embedding. However, if we have longer subpaths *on both sides* of such a vertex, then an upward planar embedding is no longer possible.

Theorem 3.27: *Let P_1 be a path containing the subgraph $\hat{P}_{\uparrow}$ illustrated in Figure 3.28a, and let P_2 be a path containing a vertex with $d_{in} = 2$. Then there is no upward planar embedding of the Cartesian product $P_1 \square P_2$. Equivalently, if P_1 contains the subgraph $\hat{P}_{\downarrow}$ illustrated in Figure 3.28b, and P_2 contains a vertex with $d_{out} = 2$, then there is also no upward planar embedding of the Cartesian product $P_1 \square P_2$.*

We only prove the first statement of the theorem; the second statement can be shown by a symmetric argument. Note that we could proceed in the same way as in Theorem 3.26, showing that the embedding of certain cycles makes an upward planar embedding impossible. However, in this case we will present a different argument, which could also have been applied in the proof of Theorem 3.26.

Proof of Theorem 3.27. We show that the Cartesian product illustrated in Figure 3.29 does not admit an upward planar embedding.

The underlying graph of this product is a grid, as illustrated in Figure 3.30a. We replace all vertices of degree 2 with a single edge, obtaining the 3-connected graph shown in Figure 3.30b. According to Whitney [Whi32], a 3-connected graph has a unique planar embedding, except for the choice of the outer face. Since we can reconstruct the original graph by subdividing edges with one vertex, the Cartesian product also has a unique planar embedding, again up to the choice of the outer face.

Figure 3.30: On the left, the Cartesian product of Figure 3.29 as a grid. On the right, the 3-connected graph we get by substituting the vertices with degree 2 with an edge.

We now demonstrate that, for every possible choice of the outer face, the resulting planar embedding is not upward. In particular, it is evident from Figure 3.30a that the depicted embedding is not upward, even if the vertex positions were rearranged. Hence, the outer face chosen in this embedding cannot yield an upward planar embedding.

Note that any face with a unique source s that has an incoming edge is unsuitable as the outer face, because the other endpoint of that incoming edge must be embedded below s. At the same time, s is the unique source of the outer face - i.e., the vertex with the lowest y-coordinate in an upward embedding. This rules out all but the faces f_0, f_3, f_4, and f_7 of Figure 3.30a.

Observe that choosing any of these faces as the outer face yields a planar embedding equivalent (up to mirroring) to choosing any of the others. Figure 3.31 illustrates the unique planar embedding with f_4 as the outer face, with vertex positions chosen to make as many edges as possible upward. Even in this optimized placement, the embedding is still not upward, regardless of how we adjust the vertex positions. Therefore, the planar embeddings with f_0, f_3, or f_7 as the outer face are also not upward.

It follows that there is no upward planar embedding for the Cartesian product in Figure 3.29, and hence no upward planar embedding for the Cartesian products of paths satisfying the conditions of Theorem 3.27.

∎

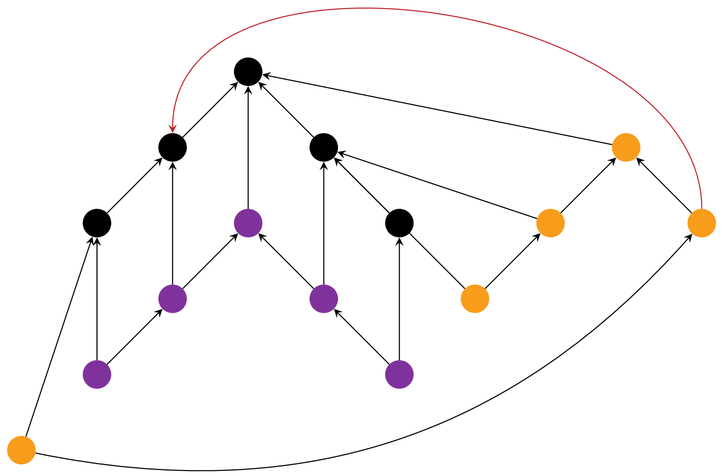

Figure 3.31: The (unique) planar embedding of Figure 3.29 with f_4 of Figure 3.30a as the outer face.

4 Posets and Upward k-Planarity

In this chapter we address another interesting graph class in the context of upward k-planarity that is given by the Hasse diagrams of posets, since the direction of the edges in a Hasse diagram is always inherently upward.

We call a poset (upward) k-planar if its Hasse diagram admits an upward k-planar embedding.

The relationship between the dimension of a poset and structural parameters of its embedding has been studied extensively. In particular, the connection between dimension and planar embeddings of Hasse diagrams has received significant attention. Baker, Fishburn and Roberts showed that a bounded poset has dimension ≤ 2 if and only if it is a 2-dimensional lattice [BFR72]. Trotter and Moore proved that the dimension of a planar poset with a greatest lower bound is at most 3 [TM77].

It is therefore natural to ask whether similar relationships can be established for upward k-planarity when $k > 0$. However, such connections do not appear to exist, as demonstrated by the following two theorems. In particular, the dimension of a poset cannot be bounded in terms of its upward local crossing number.

Theorem 4.1: *There exists no function* $f\colon \mathbb{N} \mapsto \mathbb{N}$ *such that for every upward k-planar poset* $\mathcal{P}$ *it holds that* $\dim(\mathcal{P}) \leq f(k)$.

Proof. We prove that for every $n \in \mathbb{N}$ there exists an n-dimensional poset $\mathcal{P}_n$ with $\dim(\mathcal{P}_n) = n$ and $\mathrm{lcr}^{\uparrow}(\mathcal{P}_n) = 1$.

Consider the standard example S_n. It is well known that $\dim(S_n) = n$, and that S_n is non-planar for $n \geq 5$. Thus, we start with an arbitrary upward k-planar embedding of the Hasse diagram of S_n and derive from it a new poset that remains n-dimensional but admits an upward 1-planar embedding.

Let $e_0 = uw$ be an edge that is crossed $k_0 > 1$ times. We *subdivide* e_0 exactly k_0 times, that is, at each segment between two consecutive crossings we replace a point on the edge with a new vertex. As a result, e_0 is replaced by k_0 edges, each of which is crossed at most once.

We define $\mathcal{P}_n$ as the poset whose Hasse diagram results from this subdivision process for all edges that are crossed more than one time. Importantly, subdividing an edge — i.e., for adjacent elements u, w introducing a new element v with $u < v < w$ — does not decrease the dimension of the poset because it contains the original poset still as a subposet and for every posets $\mathcal{Q}$ and subposet $\mathcal{S}$ it holds that $\dim(\mathcal{S}) \leq \dim(\mathcal{Q})$. Hence, $\dim(\mathcal{P}_n) \geq \dim(S_n) = n$.

At the same time, by construction the Hasse diagram of $\mathcal{P}_n$ admits an upward 1-planar embedding. Thus, we have $\mathrm{lcr}^{\uparrow}(\mathcal{P}_n) \leq 1$. Together, this proves the claim. ∎

We now demonstrate that the upward local crossing number cannot, in general, be bounded by a function of the dimension.

Theorem 4.2: *There exists no function* $f\colon \mathbb{N} \to \mathbb{N}$ *such that for every k-dimensional poset P it holds that* $\mathrm{lcr}^{\uparrow}(P) \leq f(k)$.

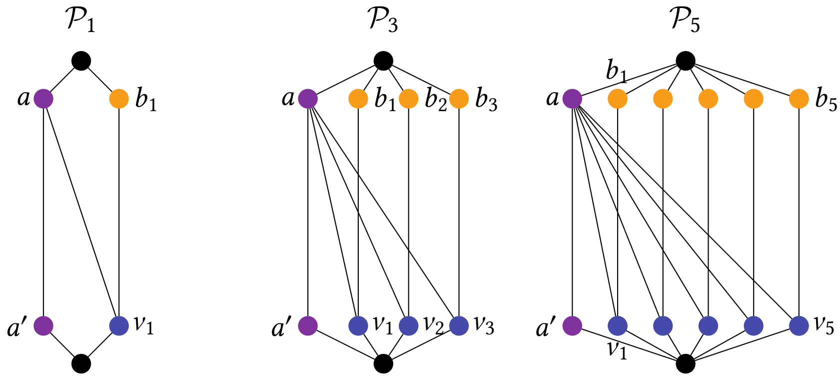

Figure 4.1: $\mathcal{P}_i$ for $i \in \{1, 3, 5\}$; The subset of elements $V_i = \{v_1, \ldots, v_i\}$ is illustrated with blue vertices, the vertices $\{a', a\}$ with violet vertices and the subset $B_i = \{b_1, \ldots, b_i\}$ with orange vertices. All edges are implicitly upward.

To prove this statement, it suffices to construct a family of posets of constant dimension whose upward local crossing number is unbounded. We explicitly define such a family and show that it satisfies these requirements. After the definition we motivate shortly, that the graphs presented in Figure 4.1 are isomorphic to the Hasse diagrams of the defined posets. The paranthesis behind the defintion of the order relation describe the visualization of the relation illustrated in Figure 4.1.

Definition 4.3: *For every $i \in \mathbb{N}$, define the poset $\mathcal{P}_i := (P_i, <_i)$ as follows. The vertex set is*

$$P_i = \{0, a', a, 1\} \cup \{v_1, \ldots, v_i\} \cup \{b_1, \ldots, b_i\}$$

and the order relation $<_i$ is given as the transitive closure of:

1. $0 < x$ *for* $x \in P_i$ *(black vertex, unique minimum)*
2. $a' < a$ *(violet vertices)*
3. $v_j < a$ *for* $j \in \{1, \ldots, i\}$ *(blue and violet vertices)*
4. $v_j < b_j$ *for* $j \in \{1, \ldots, i\}$ *(blue and orange vertices)*
5. $x < 1$ *for* $x \in P_i$ *(black vertex, unique maximum)*

We analyze whether the graphs illustrated in Figure 4.1 are isomorphic to the Hasse diagrams of the posets of Definition 4.3. Clearly, the graphs do not contain any transitive edges and have the same vertex set as the respective poset. The relations 2 - 4 in Definition 4.3 are cover relations and represented by distinct edges in each graph. Moreover, according to Definition 4.3 0 is covered only by elements in $\{a', v_1, \ldots, v_n\}$ and 1 covers only the elements in $\{a, b_1, \ldots, b_n\}$, these cover relations are also represented by edges. There are no more cover relations and the graphs in Figure 4.1 realize all the defined cover relations. Therefore, the motivated graphs are isomorphic to the respecive Hasse diagram.

		comparable pairs	incomparable pairs	Due to relation:
V_i	V_i	$\emptyset$	(v_j, v_k) for $j \neq k$	-
V_i	$\{a, a'\}$	(v_j, a)	(v_j, a')	3
V_i	B_i	(v_j, b_k) for $j = k$	(v_j, b_k) for $j \neq k$	4
$\{a\}$	$\{a'\}$	(a', a)	$\emptyset$	2
$\{a, a'\}$	B_i	$\emptyset$	$(a, b_j), (a', b_j)$	-
B_i	B_i	$\emptyset$	(b_j, b_k) for $j \neq k$	-

Table 4.1: This table sums up the comparable and incomparable elements of P_i, structured by the defined subsets. Recall that the comparability and incomparability relations are symmetrical. The last column refers to the order relations from Definition 4.3 and functions as an argument which elements from the subsets defined before are comparable. Not represented are the elements 0 and 1. Recall that these elements are comparable with all other elements in P_i.

We will now prove a series of lemmas that state that the posets $\mathcal{P}_i$ are 3-dimensional lattices and that the upward local crossing number of the Hasse diagram lies in $\Omega(i)$. This will later prove Theorem 4.2.

Our main arguments for the lemmas rely on the structure of *incomparable elements* in $\mathcal{P}_i$.

First, let us clarify which elements are comparable and which are not. Obviously, the elements $\{0, 1\} \subseteq P_i$ are comparable with every other element of P_i and the element a' is incomparable with all elements in P_i except for $\{0, a, 1\}$. Recall that comparability is a symmetric relation.

In order to analyze the comparability of the other elements $\{a, v_1, \dots, v_i, b_1, \dots, bi\}$ we define the following subsets

$$V_i = \{v_j \mid 1 \leq j \leq i\}, \qquad B_i = \{b_j \mid 1 \leq j \leq i\}.$$

With these subsets, we can furthermore analyze, that the element a is comparable to every element $v \in V_i$ and incomparable to every $b \in B_i$. For $j, k \in \{1, \dots, i\}$ the element $v_j \in V_i$ is incomparable to every $v_k \in V_i, j \neq k$ and only comparable to $b_k \in B_i$ if $j = k$, otherwise v_j incomparable to b_k. Finally, the element $b_k \in B_i$ is incomparable to every other $b_j \in B_i, j \neq k$. The relations are summarized in the Table 4.1 except for the elements $\{0, 1\}$.

So, the list of incomparable elements can be described by the fourth column of Table 4.1.

Lemma 4.4: *Every poset in the family of posets $(\mathcal{P}_i, <_i)_{i\in\mathbb{N}}$ forms a lattice.*

Proof. We prove that for every pair of elements in $\mathcal{P}_i$ there exists a unique meet and a unique join.

First, consider an element $x \in \mathcal{P}_i$ that has a unique directed path in the Hasse diagram from 0 to x. Then x has a unique meet with every element $y \in \mathcal{P}_i, x \neq y$. Indeed, if x has a unique directed path in the Hasse diagram from 0 to x, this means that $<_i$ restricted to the downset $D(x)$ is a total order. The intersection of the downset of every element $y \in \mathcal{P}_i$ $D(y)$ and $D(x)$ is not empty, since $0 \in D(x) \cap D(y)$. Among all vertices $v \in D(x) \cap D(y)$, the greatest element with respect to the order of the poset is uniquely determined by the total order of $D(x)$. Consequently, this element is the unique greatest element below both x and y, and therefore the unique meet of x and y. By a symmetric argument, if x has a unique path to 1 in the Hasse diagram, then x has a unique join with every element $y \in \mathcal{P}_i, x \neq y$.

It is straightforward to see that the elements a' and $b_1, \dots, b_i$ each admit both a unique path from 0 and a unique path to 1. Hence, each of these elements has a unique meet and join with every other element in $\mathcal{P}_i$.

Next, observe that if two elements are comparable, say $x < y$, then their meet is x and their join is y. Thus, for the analysis of $\mathcal{P}_i$ it remains to consider only incomparable pairs that do not contain any element from $\{a', b_1, \dots, b_i\}$. According to the list of incomparable elements, the only such pairs are (v_j, v_k) with $j \neq k$.

Since every $v_j \in V_i$ has a unique path from 0, each pair (v_j, v_k) has a unique meet. By inspecting the Hasse diagram, we see that the only elements greater than both v_j and v_k are a and 1, and since $a < 1$, it follows that a is their unique join.

Therefore, every pair of elements in $\mathcal{P}_i$ admits a unique meet and a unique join. Hence, $\mathcal{P}_i$ is a lattice for all $i \in \mathbb{N}$. ■

Lemma 4.5: *For the posets $(\mathcal{P}_i)_{i\in\mathbb{N}}$ it holds that* $\mathrm{lcr}^{\uparrow}(\mathcal{P}_i) \geq \frac{1}{2(3i+2)}\lfloor\frac{i}{2}\rfloor\lfloor\frac{i-1}{2}\rfloor$ *and therefore* $\mathrm{lcr}^{\uparrow}(\mathcal{P}_i) \in \Omega(i)$.

Proof. We define an auxiliary graph G_i by contracting certain edges of the Hasse diagram of $\mathcal{P}_i$ and show that $\mathrm{lcr}^{\uparrow}(G_i) \geq \frac{1}{3i+2}\lfloor\frac{i}{2}\rfloor\lfloor\frac{i-1}{2}\rfloor$. Using the structural connection of the Hasse diagram of $\mathcal{P}_i$ and G_i, we derive the lower bound for the upward local crossing number of $\mathcal{P}_i$.

Define $G_i = (P_i', E_i)$ by contracting the edges $(0, a')$ and (v_j, b_j) for $1 \leq j \leq i$ in the Hasse diagram of $\mathcal{P}_i$. Recall, that these edges exist, because they represent cover relations. For example, Figure 4.2 illustrates G_3 and G_5. For $i \in \mathbb{N}$, G_i contains the subgraph $G_i' := G_i - \{(0, a), (a, 1)\}$ whose underlying undirected graph is isomorphic to the complete bipartite graph $K_{3,i}$. This is illustrated in Figure 4.3.

Is is already shown by Kleitmann[Kle70], that the crossing number of $K_{m,n}$ is given by $cr(K_{m,n}) = \lfloor\frac{m}{2}\rfloor\lfloor\frac{m-1}{2}\rfloor\lfloor\frac{n}{2}\rfloor\lfloor\frac{n-1}{2}\rfloor$ for $m \leq 6$. Therefore, $cr(K_{3,i}) = \lfloor\frac{3}{2}\rfloor\lfloor\frac{2}{2}\rfloor\lfloor\frac{i}{2}\rfloor\lfloor\frac{i-1}{2}\rfloor = \lfloor\frac{i}{2}\rfloor\lfloor\frac{i-1}{2}\rfloor$.

For a subgraph H of a graph G it holds that $cr(G) \geq cr(H)$, so we can derive that $cr(G_i) \geq cr(G_i') = cr(K_{3,i}) = \lfloor\frac{i}{2}\rfloor\lfloor\frac{i-1}{2}\rfloor$.

It holds that $|E_i| = 3i + 2$. That means there has to be at least one edge $e \in E_i$ that has at least $\frac{1}{3i+2}cr(G_i)$ crossings, therefore the local crossing number of G_i is at least $\frac{1}{3i+2}\lfloor\frac{i}{2}\rfloor\lfloor\frac{i-1}{2}\rfloor$.

With the fact that $\mathrm{lcr}^{\uparrow}(G) \geq \mathrm{lcr}(G)$ for every directed graph G, we derive $\mathrm{lcr}^{\uparrow}(G_i) \geq \mathrm{lcr}(G_i) \geq \frac{1}{3i+2}\lfloor\frac{i}{2}\rfloor\lfloor\frac{i-1}{2}\rfloor$.

Since G_i is constructed by the contraction of edges of the Hasse diagram of $\mathcal{P}_i$, where at least one endpoint has a vertex degree of 2, we can reconstruct the Hasse diagram by subdividing certain edges. In particular, we have to subdivide the edges $(0, a), (v_1, 1), \dots (v_i, 1)$ once.

Since every edge in G_i is only divided into at most two new edges to create the Hasse diagram of $\mathcal{P}_i$, the crossing per edge are also divided by at most two. Consequently, $\mathrm{lcr}^{\uparrow}(\mathcal{P}_i) \geq \frac{1}{2}\,\mathrm{lcr}^{\uparrow}(G_i) \geq \frac{1}{2(3i+2)}\lfloor\frac{i}{2}\rfloor\lfloor\frac{i-1}{2}\rfloor$. ■

Lemma 4.6: *Every poset in the family of posets $(\mathcal{P}_i, <_i)_{i\in\mathbb{N}}$ has dimension* 3.

Proof. First, we define three linear extensions and show that $\dim(\mathcal{P}_i) \leq 3$, and then argue for equality.

Define the linear extensions

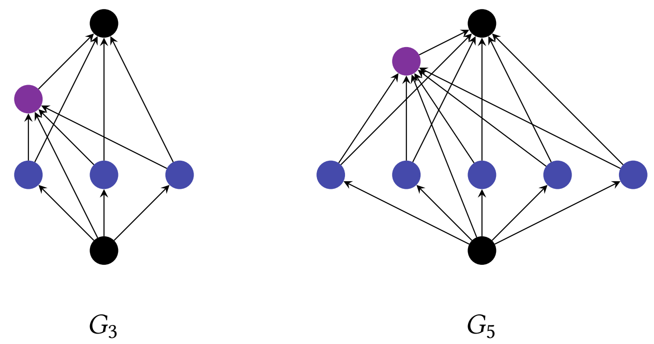

Figure 4.2: This illustrates the auxiliray graphs G_3 and G_5. The vertices v_j are illustrated in blue, the vertex a is illustrated in violet, 0 and 1 as a black vertex at the bottom and top, respectively. We can construct the Hasse diagrams from Figure 4.1 by subdividing the edges from the blue vertices to 1 and the edge from a to 0. .

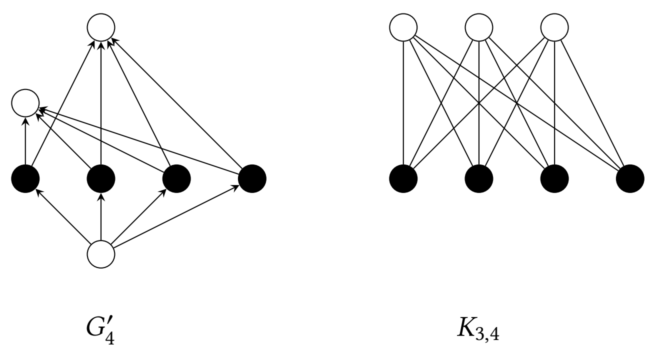

Figure 4.3: This figure illustrates the graph G'_4 on the left, whose underlying undirected graph is isomorphic to $K_{3,4}$ on the right. The coloring of the vertices motivates the isomorphism.

$$\ell_{1(i)} = 0, v_1, b_1, v_2, b_2, \dots, v_i, b_i, a', a, 1;$$
$$\ell_{2(i)} = 0, v_i, b_i, v_{i-1}, b_{i-1}, \dots, v_1, b_1, a', a, 1;$$
$$\ell_{3(i)} = 0, a', v_1, v_2, \dots, v_i, a, b_1, b_2, \dots, b_{i-1}, 1.$$

We claim that $\ell_{1(i)} \cap \ell_{2(i)} \cap \ell_{3(i)} = \mathcal{P}_i$. It is straightforward to verify that these three linear extensions respect all order relations specified in Definition 4.3. What remains is to show that all pairs of incomparable elements in $\mathcal{P}_i$ remain incomparable under the intersection.

For and $j, k \in \{1, \dots, i\}$, $j \neq k$:

- (v_j, v_k) for $k \neq j$ are incomparable due to $\ell_{1(i)} \cap \ell_{2(i)}$,
- (v_j, a') are incomparable due to $\ell_{1(i)} \cap \ell_{3(i)}$,
- (v_j, b_k) for $k \neq j$ are incomparable due to $\ell_{1(i)} \cap \ell_{2(i)}$,
- (a, b_j) are incomparable due to $\ell_{1(i)} \cap \ell_{3(i)}$,
- (a', b_j) are incomparable due to $\ell_{1(i)} \cap \ell_{3(i)}$ and
- (b_k, b_j) are incomparable due to $\ell_{1(i)} \cap \ell_{2(i)}$.

Hence, $\dim(\mathcal{P}_i) \leq 3$.

As established in Lemma 4.5, the Hasse diagram of $\mathcal{P}_i$ is not planar and $\mathcal{P}_i$ is a lattice. By the result of Baker, Fishburn and Roberts [BFR72], it follows that $\dim(\mathcal{P}_i) > 2$. Thus, $\dim(\mathcal{P}_i) = 3$. ∎

Proof of Theorem 4.2. This follows directly the properties of the poset family $(\mathcal{P}_i)_{i \in \mathbb{N}}$ that were proven in Lemma 4.4, Lemma 4.5 and Lemma 4.6. ∎

5 Conclusion

The main focus of this thesis is to investigate whether it is possible to establish improved bounds for the upward local crossing number of graph classes with a fixed edge orientation.

We show that such improved bounds can indeed be formulated, both for Cartesian products of upward k-planar graphs in general and for Cartesian products of orientated paths in particular. Since the bound obtained for the Cartesian product of paths is stronger than the improved bound for general Cartesian products of upward k-planar graphs, this suggests that improved bounds may also be found for other specific Cartesian products. Given that the local crossing number of Cartesian products of cycles and stars has also been studied in the undirected case [Mus19], it would be of interest to investigate the upward local crossing number of these Cartesian products and to compare the results with those known for the undirected setting.

Unfortunately, we were not able to establish a general lower bound for Cartesian products. In the case of Cartesian products of paths, our analysis was limited to identifying the conditions under which $lcr(P_1 \square P_2) > 0$. Hence, deriving stronger lower bounds for Cartesian products of paths as well as for upward k-planar graphs remains an open and interesting problem. Initial arguments in this direction could be developed by establishing a lower bound for the bandwidth of orientated paths.

Our analysis of Cartesian products demonstrates that it is possible to obtain better bounds depending on the choice of the input graphs. Another promising research direction would be to study other graph products, such as the strong product, to formulate upper bounds, and to compare embedding techniques in terms of their ability to minimize the upward local crossing number. It would also be interesting to explore potential relationships between the upward local crossing number of Cartesian products and that of other graph products on the same input graphs.

In Chapter 4 we observed that the upward local crossing number of posets does not appear to be related to the dimension of the poset. Since many poset parameters are typically connected to dimension, it may be difficult to identify a parameter that directly correlates with the upward local crossing number. Nevertheless, it may be worthwhile to study lower bounds for the upward local crossing number based on structural patterns in the partial order or on other combinatorial properties of the poset. Determining the upward local crossing number of specific posets, such as the standard example S_n or the Boolean lattice B_n, could provide a deeper understanding of the relationship between the upward local crossing number and the combinatorial properties of posets.

Another possible approach for combining posets with upward k-planarity would be to analyze the upward local crossing number of comparability or incomparability graphs instead of the Hasse diagrams.

Bibliography

[Ang+25] Patrizio Angelini, Therese Biedl, Markus Chimani, Sabine Cornelsen, Giordano Da Lozzo, Seok-Hee Hong, Giuseppe Liotta, Maurizio Patrignani, Sergey Pupyrev, Ignaz Rutter, and Alexander Wolff. "The Price of Upwardness". In: *Discrete Mathematics amp; Theoretical Computer Science* Volume 27:3 (Aug. 2025). ISSN: 1365-8050. DOI: *10.46298/dmtcs.15222*.

[Asi+24] Zayed Asiri, Ryan Burdett, Markus Chimani, Michael Haythorpe, Alex Newcombe, and Mirko H. Wagner. *A Systematic Approach to Crossing Numbers of Cartesian Products with Paths*. 2024. arXiv: *2409.06755*.

[Bek20] Michael A. Bekos. "k-Planar Graphs". In: *Beyond Planar Graphs: Communications of NII Shonan Meetings*. Edited by Seok-Hee Hong and Takeshi Tokuyama. Singapore: Springer Singapore, 2020, pp. 109–130. ISBN: 978-981-15-6533-5. DOI: *10.1007/978-981-15-6533-5_7*.

[BFR72] K. A. Baker, P. C. Fishburn, and F. S. Roberts. "Partial orders of dimension 2". In: *Networks* Volume 2 (1972), pp. 11–28. DOI: *10.1002/net.3230020103*.

[CDGK75] J. Chvatalova, A.K. Dewdney, N.E. Gibbs, and R.R. Korfhage. "The bandwidth problem for graphs: a collection of recent results". In: *Research Report 24, Department of Computer Science, UWO, London* (1975).

[DGL10] Walter Didimo, Francesco Giordano, and Giuseppe Liotta. "Upward Spirality and Upward Planarity Testing". In: *SIAM Journal on Discrete Mathematics* Volume 23 (2010), pp. 1842–1899. DOI: *10.1137/070696854*.

[DLM19] Walter Didimo, Giuseppe Liotta, and Fabrizio Montecchiani. "A Survey on Graph Drawing Beyond Planarity". In: *ACM Comput. Surv.* Volume 52 (Feb. 2019). ISSN: 0360-0300. DOI: *10.1145/3301281*.

[DM41] Ben Dushnik and E. W. Miller. "Partially Ordered Sets". In: *American Journal of Mathematics* Volume 63 (1941), pp. 600–610. DOI: *10.2307/2371374*.

[DT88] Giuseppe Di Battista and Roberto Tamassia. "Algorithms for plane representations of acyclic digraphs". In: *Theoretical Computer Science* Volume 61 (1988), pp. 175–198. ISSN: 0304-3975. DOI: *10.1016/0304-3975(88)90123-5*.

[GT01] Ashim Garg and Roberto Tamassia. "On the Computational Complexity of Upward and Rectilinear Planarity Testing". In: *SIAM Journal on Computing* Volume 31 (2001), pp. 601–625. DOI: *10.1137/S0097539794277123*.

[KA02] Toru Kojima and Kiyoshi Ando. "Bandwidth of the cartesian product of two connected graphs". In: *Discrete Mathematics* Volume 252 (2002), pp. 227–235. ISSN: 0012-365X. DOI: *10.1016/S0012-365X(01)00455-1*.

[Kle70] Daniel J. Kleitman. "The crossing number of K5,n". In: *Journal of Combinatorial Theory* Volume 9 (1970), pp. 315–323. ISSN: 0021-9800. DOI: *10.1016/S0021-9800(70)80087-4*.

[Mus19] Marine Musulyan. “Local Crossing Numbers of the Product of Planar Graphs and Cycles”. California State University, Northridge, May 2019. eprint: *https://scholarworks.calstate.edu/downloads/rx913s972*.

[Sch18] Marcus Schaefer. *Crossing Numbers of Graphs*. 1st. CRC Press, 2018. DOI: *10.1201/9781315152394*.

[SV91] Ondrej Sýkora and Imrich Vrto. *On Crossing Numbers of Hypercubes and Cube Connected Cycles*. Saarbrücken: Max-Planck-Institut für Informatik, 1991. DOI: *10.1007/bf01989746*.

[TM77] William T Trotter and John I Moore. “The dimension of planar posets”. In: *Journal of Combinatorial Theory, Series B* Volume 22 (1977), pp. 54–67. ISSN: 0095-8956. DOI: *10.1016/0095-8956(77)90048-X*.

[Whi32] Hassler Whitney. “Congruent Graphs and the Connectivity of Graphs”. In: *American Journal of Mathematics* Volume 54 (1932), pp. 150–168. ISSN: 00029327, 10806377. DOI: *10.2307/2371086*.